

Supporting Information

Strongly fluorescent indolizine-based coumarin analogs

Jaqueline S. A. Badaro,^a Antoni Wrzosek,^b Olaf Morawski,^c Adam Szewczyk,^{*b} Irena Deperasińska,^{*c} and Daniel T. Gryko,^{*a}

^a*Institute of Organic Chemistry, Polish Academy of Sciences, Kasprzaka 44/52, 01-224 Warsaw, Poland.*

^b*Nencki Institute of Experimental Biology, Polish Academy of Sciences, Pasteur 3, 02-093 Warsaw, Poland.*

^c*Institute of Physics, Polish Academy of Sciences, Al. Lotników 32/46, 02-668 Warsaw, Poland*

Table of Contents

1. Computational Details	2
2. Photophysical measurements	12
3. Imaging Studies	22
4. ¹H NMR and ¹³C NMR spectra	23

1. Computational Details

Table S1. Absorption and fluorescence energies and their oscillator strengths for molecules in DMSO solution calculated using the M06 and O3LYP functionals along with experimental data.

Solvent: DMSO		experiment	M06/6-31G(d,p)		O3LYP/6-31G(d,p)	
molecule	transition	E [nm]	E [nm]	f	E [nm]	f
2b	abs	449	407	0.7423	422	0.6367
	flu	481	437	0.6599	470	0.3896
2a	abs	444	402	0.7657	417	0.6591
	flu	475	428	0.6903	460	0.4231
2c	abs	466	423	0.6749	440	0.5488
	flu	503	465	0.5339	512	0.3075
3aa	abs	451	417	0.6453	437	0.5194
	flu	501	456	0.5153	500	0.3112
4a	abs	426	387	0.7439	404	0.6500
	flu	447	410	0.7205	434	0.5071
3ac	abs	457	430	0.5785	452	0.4327
	flu	521	489	0.3933	545	0.2278
6a	abs	500	488	1.1948	526	1.0633
	flu	594	520	1.2776	552 895 ^a	1.0173 0.0000
3ab	abs	448	439	0.6547	518	0.3756
	flu	492/702	505	0.5520	762 ^a	0.0000

^a dark conformer (see Figs.S7 and S8)

Table S2. Summary of experimental and calculated (using the TD O3LYP/6-31G(d,p) method) absorption and fluorescence energies in solvents of different polarity: toluene, DCM, and DMSO. All values in [nm]. The calculated

values characterize structures previously optimized in the ground states S_0 and the lowest electronically excited S_1 , respectively.

TOLUE					cal	
NE						
	abs-exp	abs-cal	flu-exp	flu-cal		
2b	449	401	464	468		
2a	441	395	457	454		
2c	467	419	486	511		
2e	457	420	467	455		
2f	436	401	450	479		
2i	454	425	480	537		
4a	428	388	444	432		
3aa	452	420	480	507		
3ac	454	437	501	555		
3ab	452	472	477	680		
DCM					cal	
2b	449	416	470	468		
2a	446	410	464	458		
2c	468	434	494	511		
2e	456	435	470	470		
2f	436	416	458	486		
2i	446	435	485	508		
4a	426	400	448	432		
3aa	453	431	490	500		
3ac	457	447	514	547		
3ab	452	505	642	736		
6a	509	526	575	563		
DMSO					cal	
2b	449	422	481	470		
2a	444	417	475	460		
2c	466	440	503	512		
2e	456	441	478	476		
2f	437	422	473	490		
2i	448	440	493	502		
4a	426	404	447	434		
3aa	451	437	501	500		
3ac	457	452	521	545		
3ab	448	518	702	762		
6a	500	526	594	552		

Table S3. Values of the calculated dipole moments (in [D]) in the ground S_0 and excited S_1 states of the molecules in DMSO.

	$\mu(S_0)$	$\mu(S_1)$
2b	9.6	12.0
2a	10.0	12.5
2c	9.7	12.2
2e	9.7	10.6
2f	9.7	13.9
2i	15.1	17.1
4a	9.9	11.2
3aa	13.1	13.7
3ac	9.7	13.7
3ab	13.4	31.7
6a	22.3	15.5

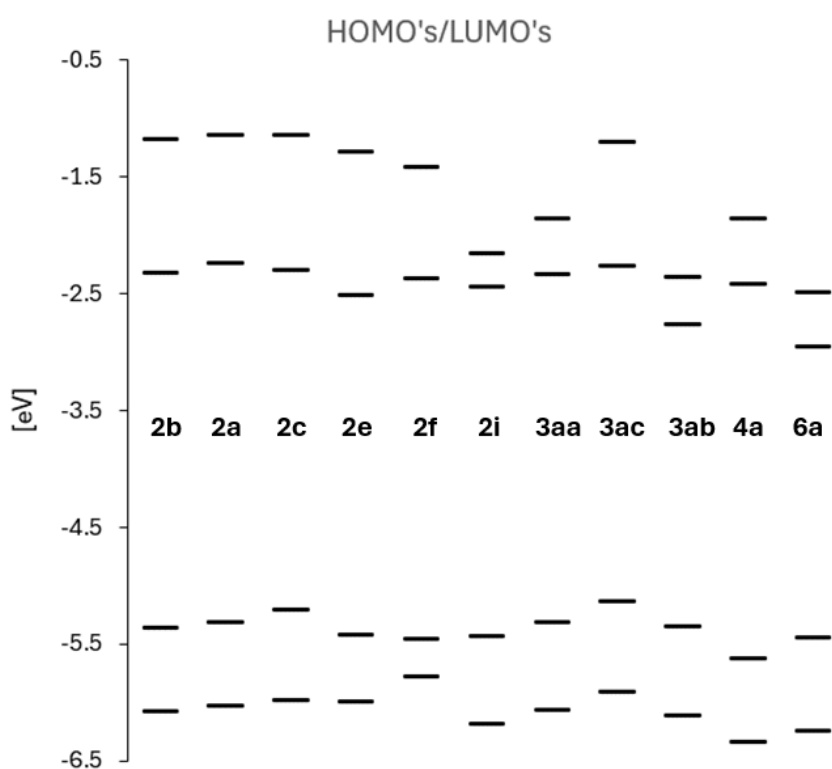


Figure S1. Energies of four frontier orbitals (HOMO-1, HOMO, LUMO, LUMO+1) for the molecules of the studied group. In each case, Substitution 2b leads to shifts of all rungs in the corresponding ladders.

Table S4. Tested compounds ranked according to HOMO (part A) and LUMO (part B) energies [all data in eV]. Part C – Values of $\Delta_H = \text{HOMO} - \text{HOMO}(2b)$ and $\Delta_L = \text{LUMO} - \text{LUMO}(2b)$ for individual molecules

A	HOMO	$\Delta_H = \text{HOMO} - \text{HOMO}(2b)$	LUMO
4a	-5.62	-0.26	-2.42
2f	-5.46	-0.10	-2.38
6a	-5.44	-0.08	-2.95
2i	-5.43	-0.07	-2.45
2e	-5.42	-0.06	-2.51
2b	-5.36	0.00	-2.33
3ab	-5.35	0.01	-2.77
2a	-5.31	0.05	-2.24
3aa	-5.31	0.05	-2.34
2c	-5.21	0.15	-2.29
3ac	-5.14	0.22	-2.26

B	HOMO	LUMO	$\Delta_L = \text{LUMO} - \text{LUMO}(2b)$
6a	-5.44	-2.95	-0.62
3ab	-5.35	-2.77	-0.44
2e	-5.42	-2.51	-0.19
2i	-5.43	-2.45	-0.12
4a	-5.62	-2.42	-0.09
2f	-5.46	-2.38	-0.05
3aa	-5.31	-2.34	-0.01
2b	-5.36	-2.33	0.00
2c	-5.21	-2.29	0.03
3ac	-5.14	-2.26	0.07
2a	-5.31	-2.24	0.09

C	Δ_H	Δ_L
2a	0.05	0.09
3ac	0.22	0.07
2c	0.15	0.03
2b	0.00	0.00
3aa	0.05	-0.01
2f	-0.10	-0.05
4a	-0.26	-0.09
2i	-0.07	-0.12
2e	-0.06	-0.19
3ab	0.01	-0.44
6a	-0.08	-0.62

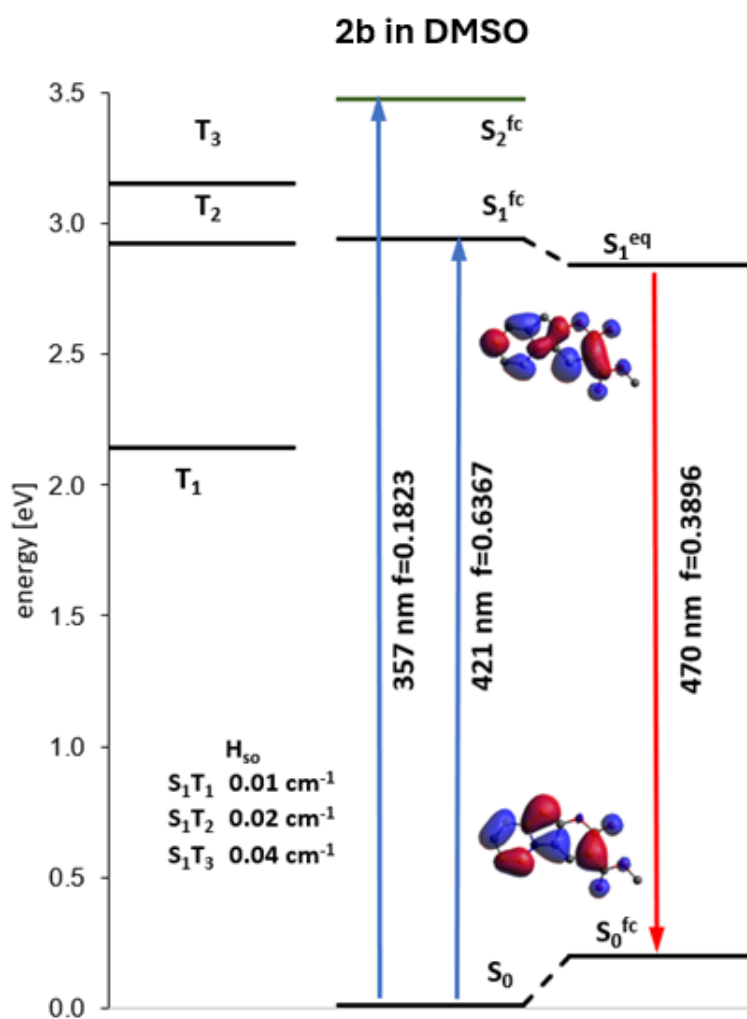
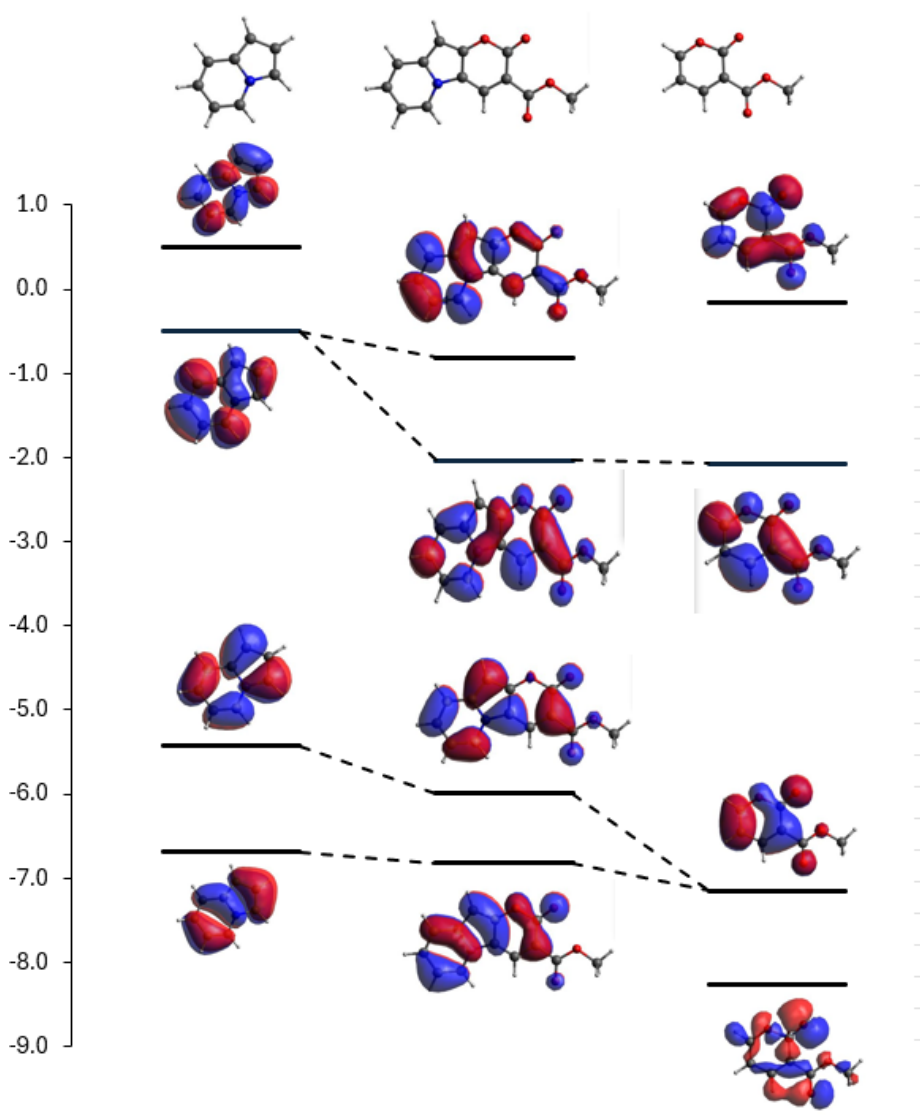


Figure S2. Diagram of the electronic states of **2b** in DMSO. The states S_0 , S_1^{eq} correspond to the energy minimum. States marked with “fc” are the final (Franck-Condon) states in vertical absorption and fluorescence. Next to the arrows corresponding to these transitions, the energy and oscillator strength values that characterize them are given. The shapes of HOMO and LUMO orbitals, describing transition between S_0 and S_1 states are shown. The interactions between the S_1 state and the lowest triplet T_i states are described by small value SOC elements. The energy change in the relaxation process $S_1^{fc} \rightsquigarrow S_1^{eq}$ is ~ 0.1 eV. This process takes place in the excited state but in essence it is the adaptation of the molecular structure of the S_0 state to the new charge distribution created by the excitation. The small changes in the geometry are also reflected by the calculated vibrational structure of the **2b** fluorescence spectrum (next Fig. S3) built on a framework of Franck-Condon factors with small values.



TD DFT M06/6-31G(d,p)/ DFT M06/6-31G(d,p)		
DMSO		
IND	2b = IND-COUM	COUM
3.782 eV f=0.105	3.045 eV f=0.742	4.065 eV f=0.320

Figure S3. **2b** as a combination of indolizine and coumarin frontier orbitals. Absorption energies and oscillator strengths. Transition moment vectors

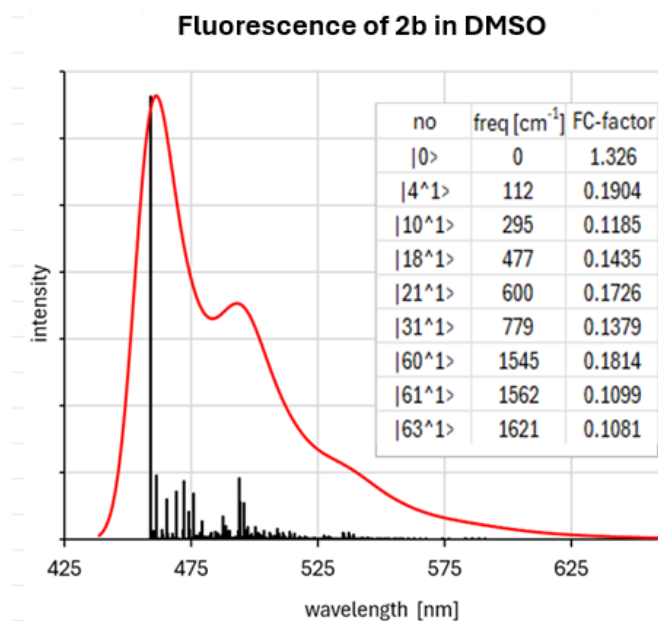


Figure S4. Simulation of **2b** fluorescence spectrum in DMSO. The attached table shows the values of the Franck-Condon factors for most active vibrational modes. The corresponding lines have been widened with $fwch = 200 \text{ cm}^{-1}$. The simulated spectrum reproduces the experimental spectrum well.

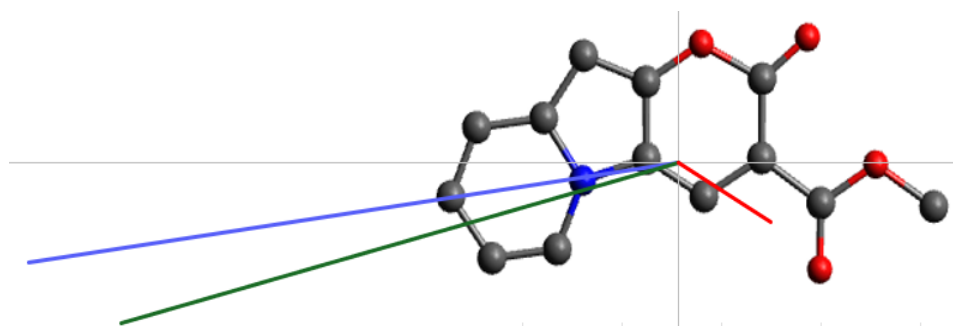


Figure S5. The directions of the dipole moment vectors in the ground state $\mu(S_0)$ (green), the excited state $\mu(S_1)$ (blue) and the direction of vector their vector difference $\Delta\mu = \mu(S_1) - \mu(S_0)$ (red). According to the classical theory of the solvent effect,⁶⁰ the absorption and fluorescence energies in solvent, described by dielectric constant ϵ , are given as:

$$E_{abs}(\epsilon) = E_{abs}(isol) - \alpha\mu(S_0) \Delta\mu f(\epsilon)$$

$$E_{flu}(\epsilon) = E_{flu}(isol) - \alpha\mu(S_1) \Delta\mu f(\epsilon)$$

where $E_{abs}(isol)$ and $E_{flu}(isol)$ are absorption and fluorescence energies of isolated molecule, $\alpha=const$, $f(\epsilon)$ is solvent polarity function. Therefore, the shifts of absorption and fluorescence are dependent on the scalar products between two vectors $\mu(S_0) \Delta\mu$ and $\mu(S_1) \Delta\mu$, respectively. The value of scalar products of two vectors is dependent on the cosine of the angle between these vectors. Hence, the angle between red vector ($\Delta\mu$) and the blue vector ($\mu(S_1)$) is large, then cosine is small and fluorescence shift is small and, according to this approach, the absorption shift is even smaller (described by products of the green and red vectors).

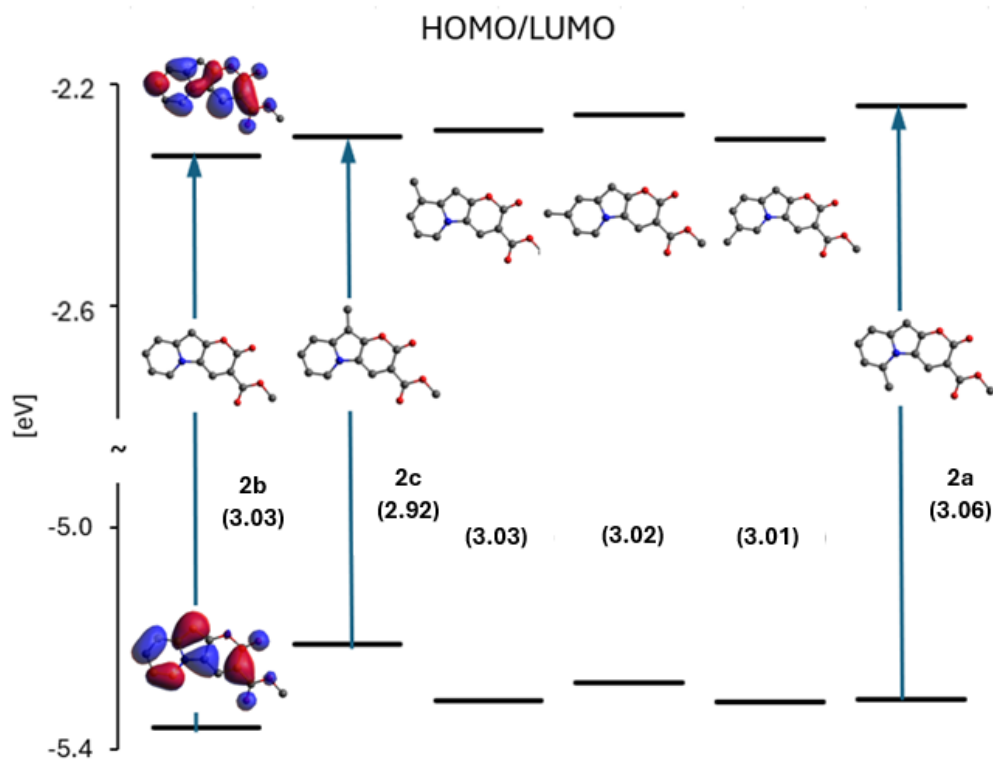


Figure S6. HOMO and LUMO energy changes with methylation of **2b** at different positions.

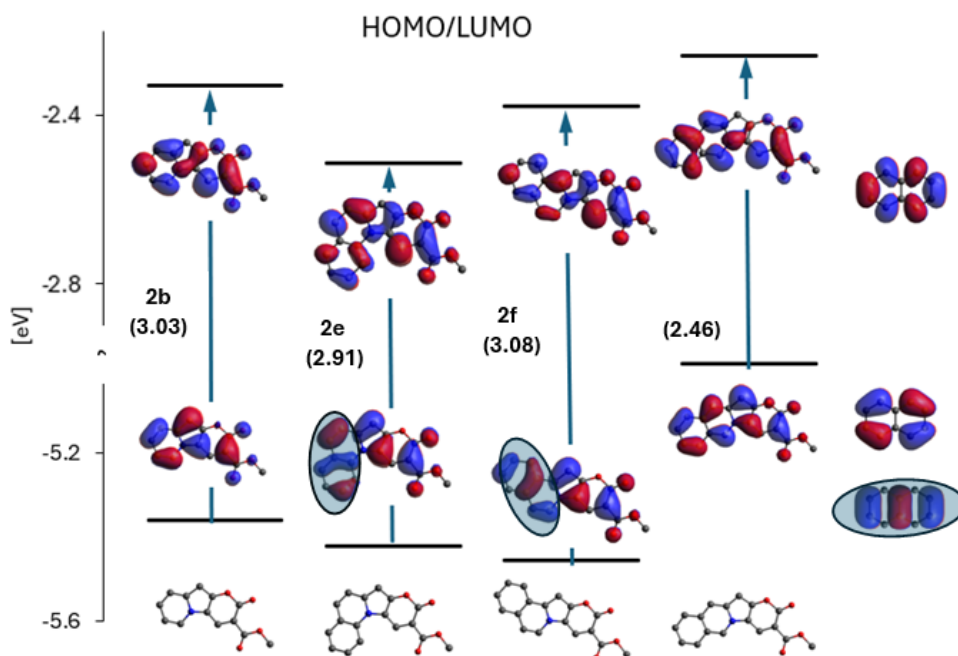


Figure S7. Changes in the energy and shape of HOMO and LUMO at different expansions **2b**. From a topological look at the shape of the orbitals, one can notice the deformed naphthalene part (isolated naphthalene orbitals on the right side) in the HOMO and LUMO of extended molecules. For the third possible expansion mode, the HOMO of molecule **2b** would mix with a different naphthalene orbital than in the previous cases.

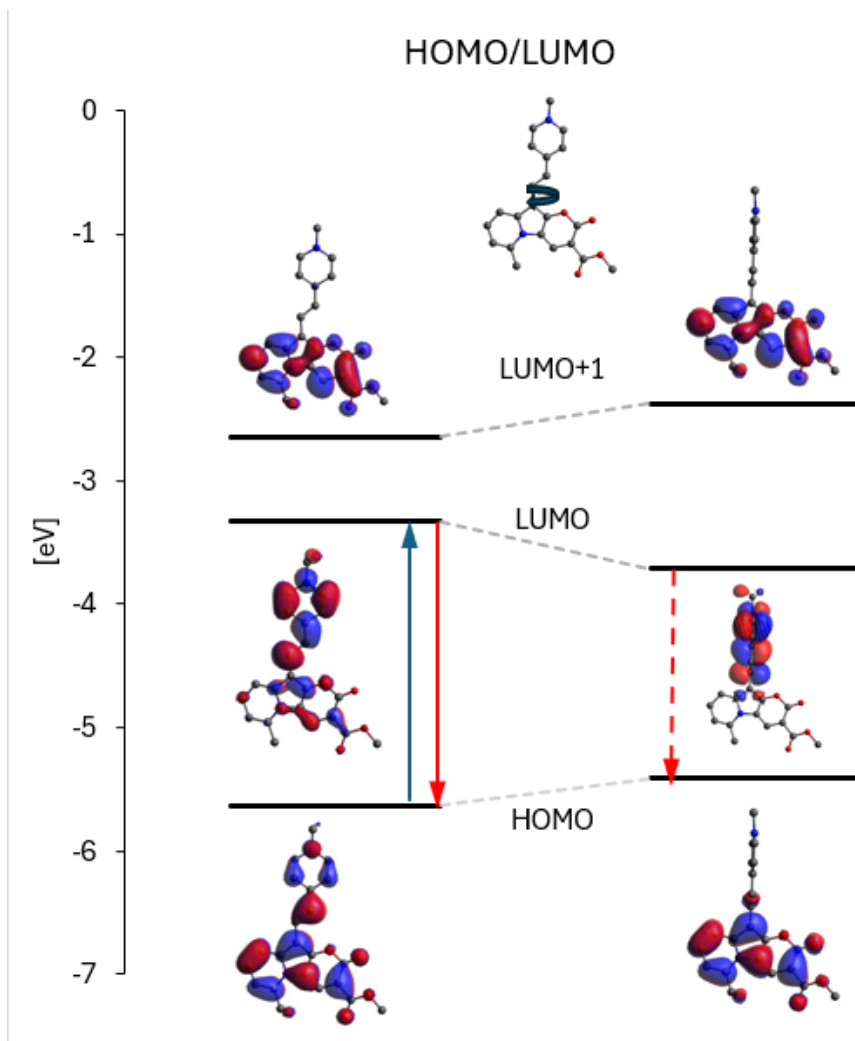


Figure S8. HOMO and LUMO of bright and dark forms of **6a**.

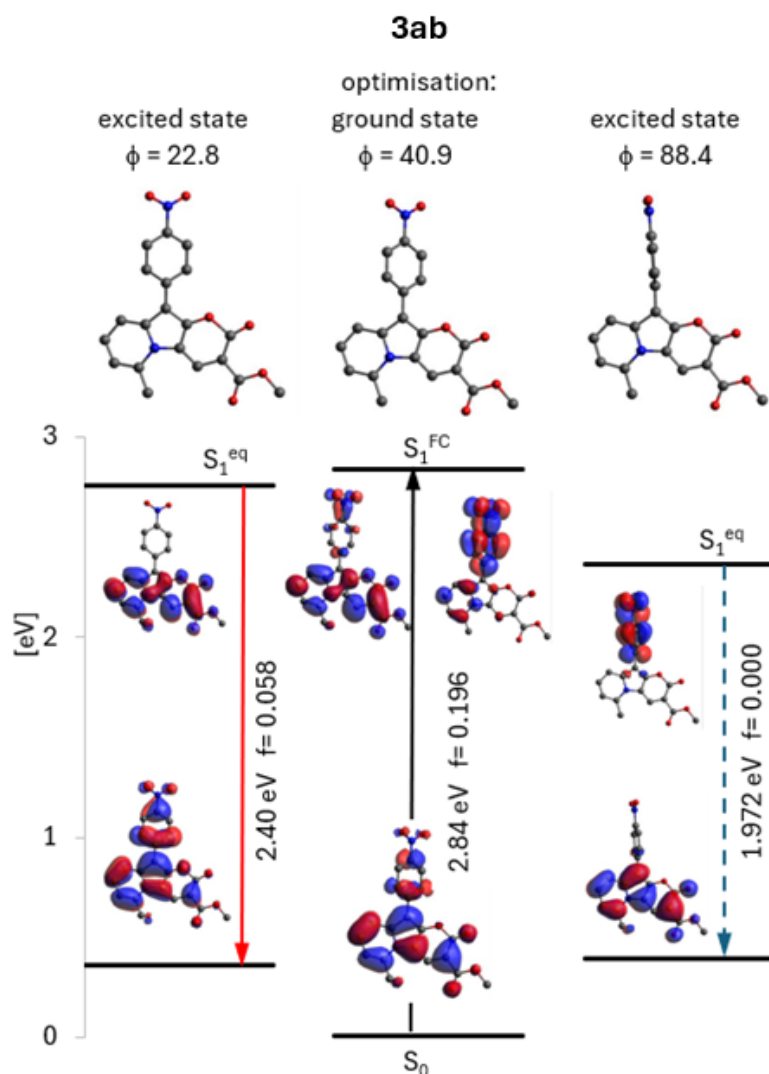
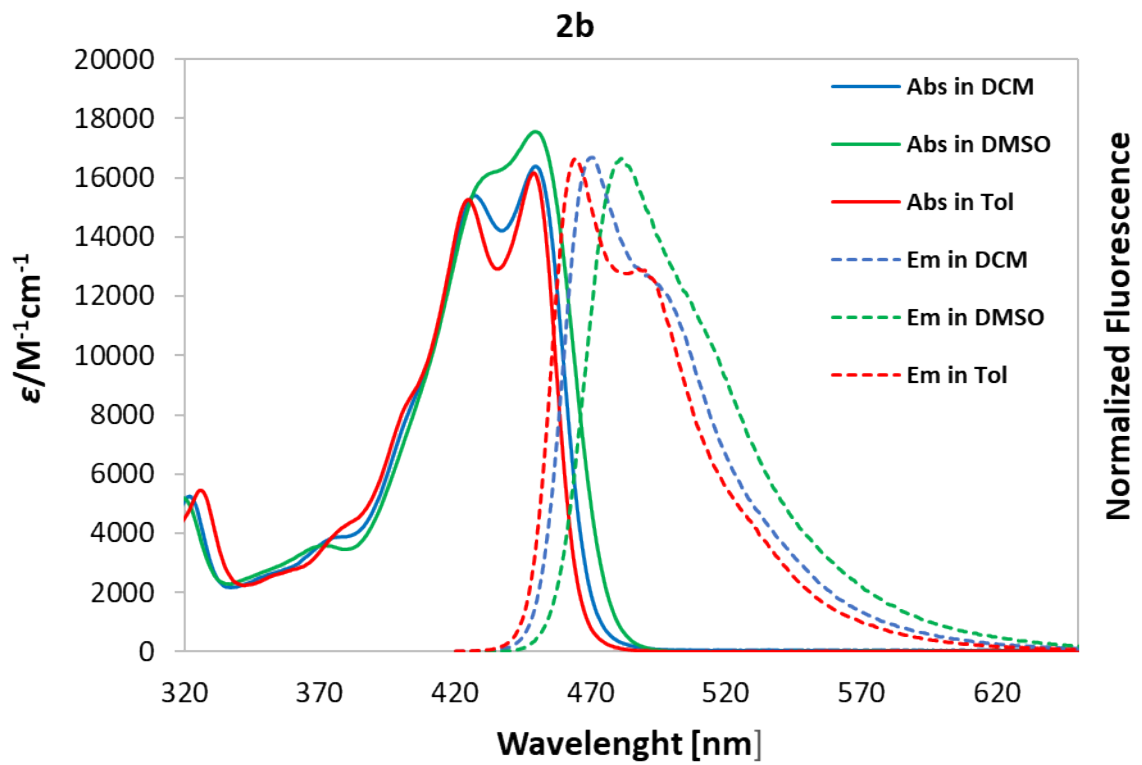
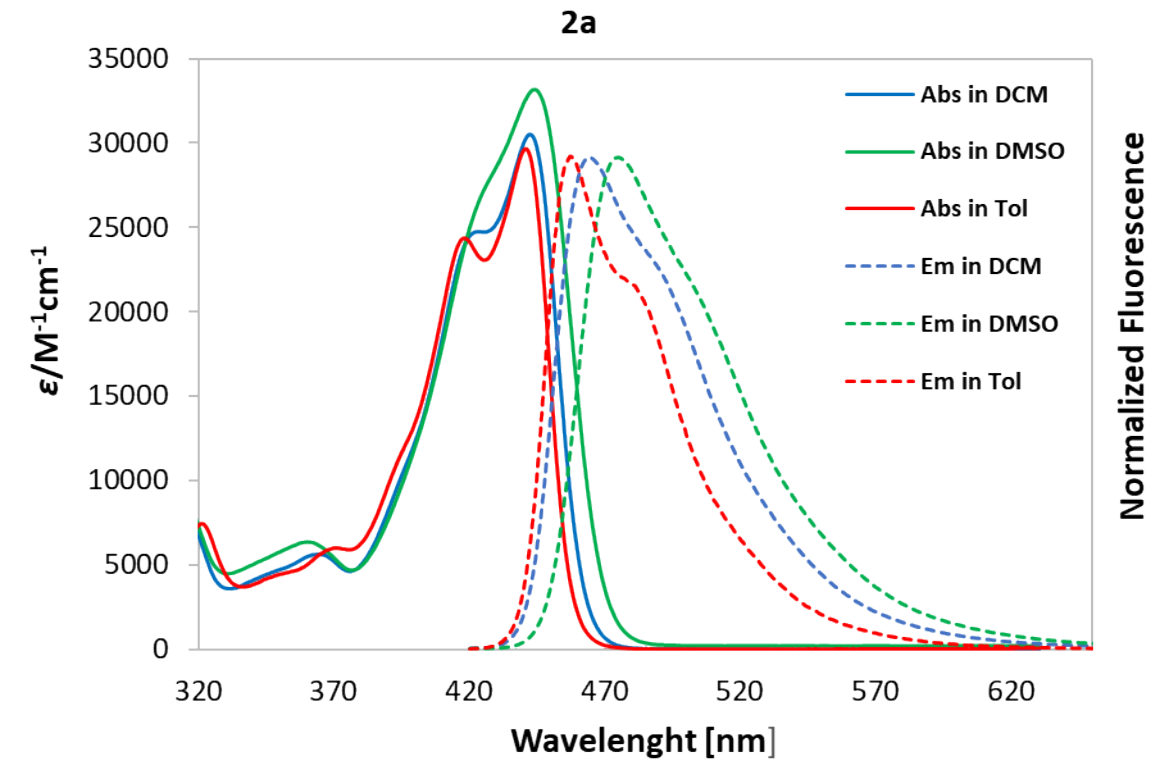


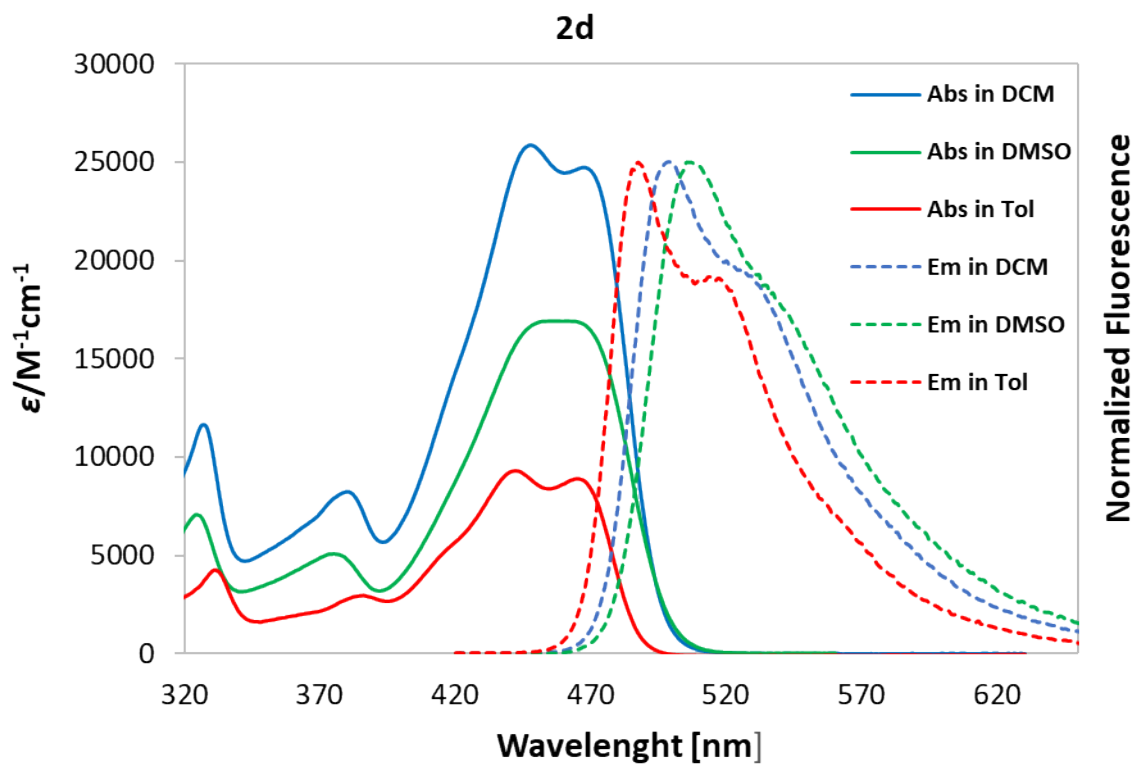
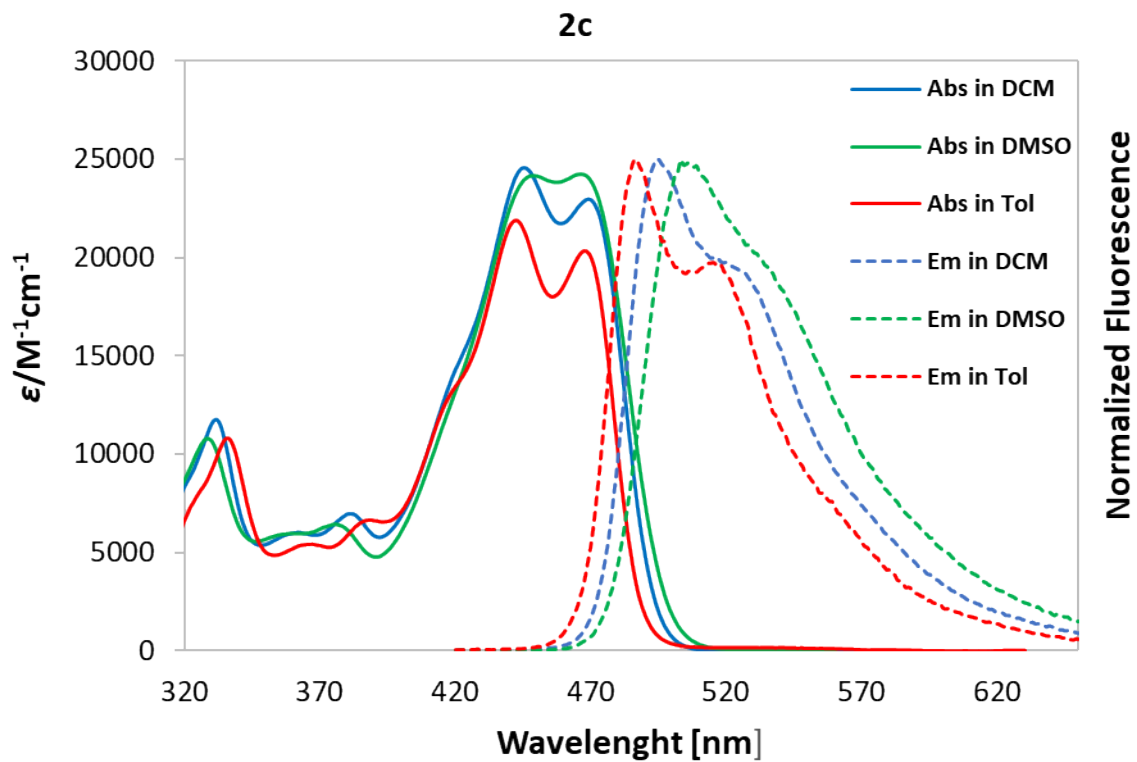
Figure S9. Electronic states of 3ab. (left and right) Energies and configurations of 3ab in two minima optimized in the electronically excited S_1 state. (center) Energetics 3ab for geometry optimized in the S_0 ground state. Electronic excitation leads to the S_1^{FC} state described by a combination of two electron configurations HOMO/LUMO(2b) and HOMO/LUMO'(sub). Relaxation of S_1^{FC} leads to two energy minima, corresponding to bright and dark form. The emission of bright form is the emission characteristic of the studied family of molecules. However, in the second minimum the molecule is in the dark state, as the oscillator strength is zero because of the lack of overlap between LUMO' and HOMO.

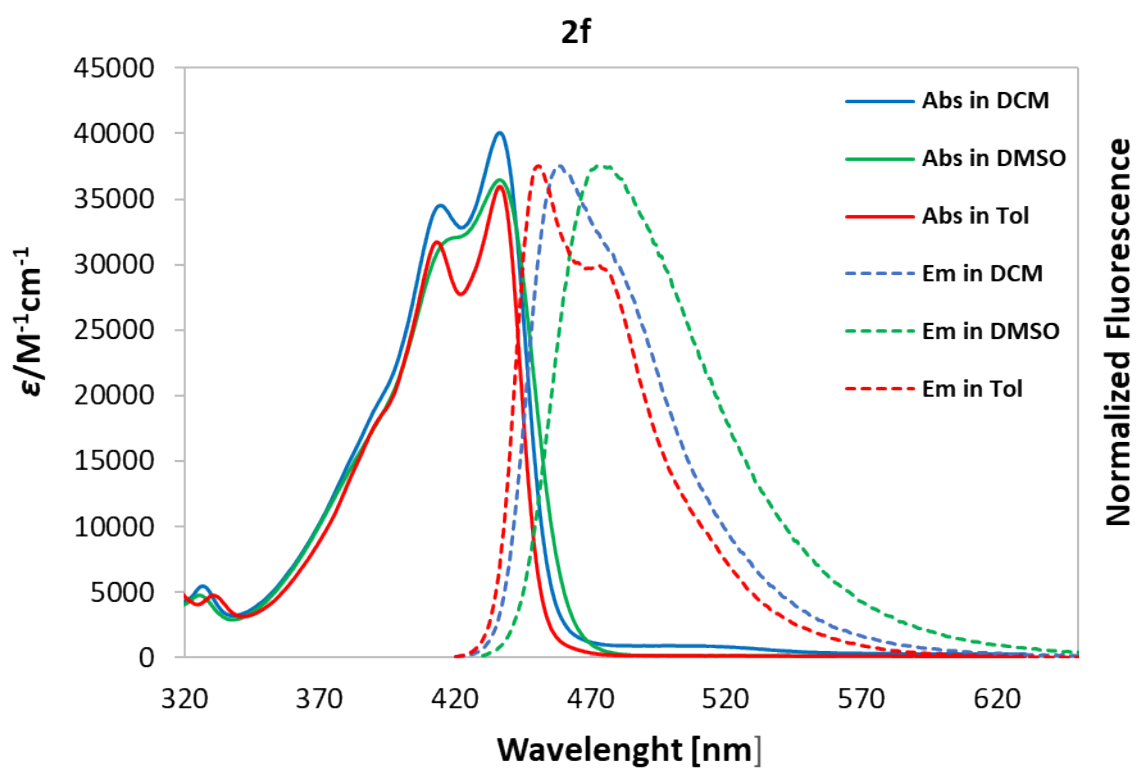
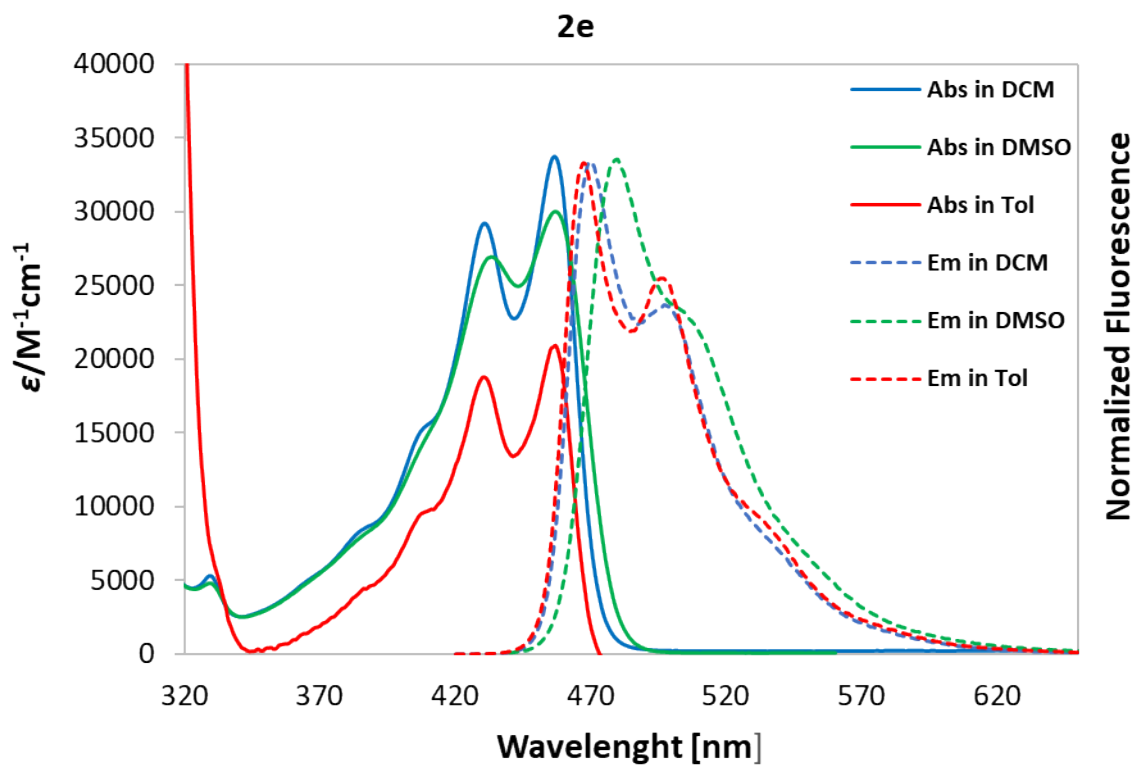
2. Photophysical Measurements

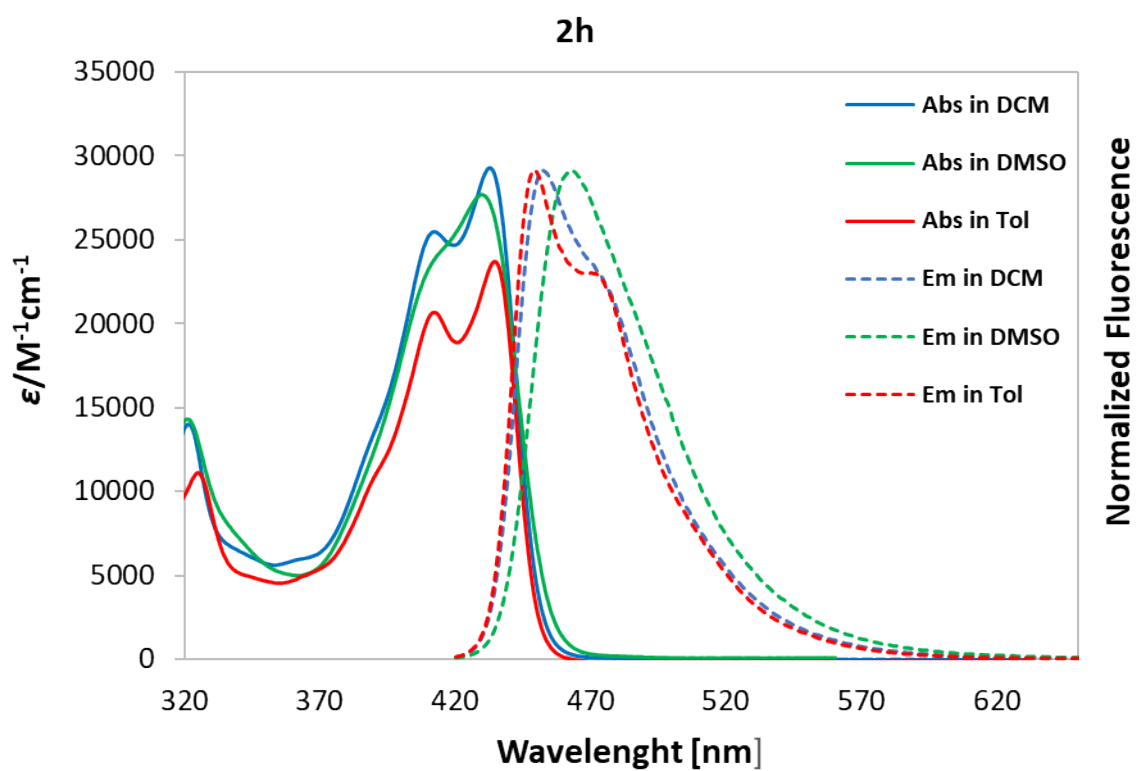
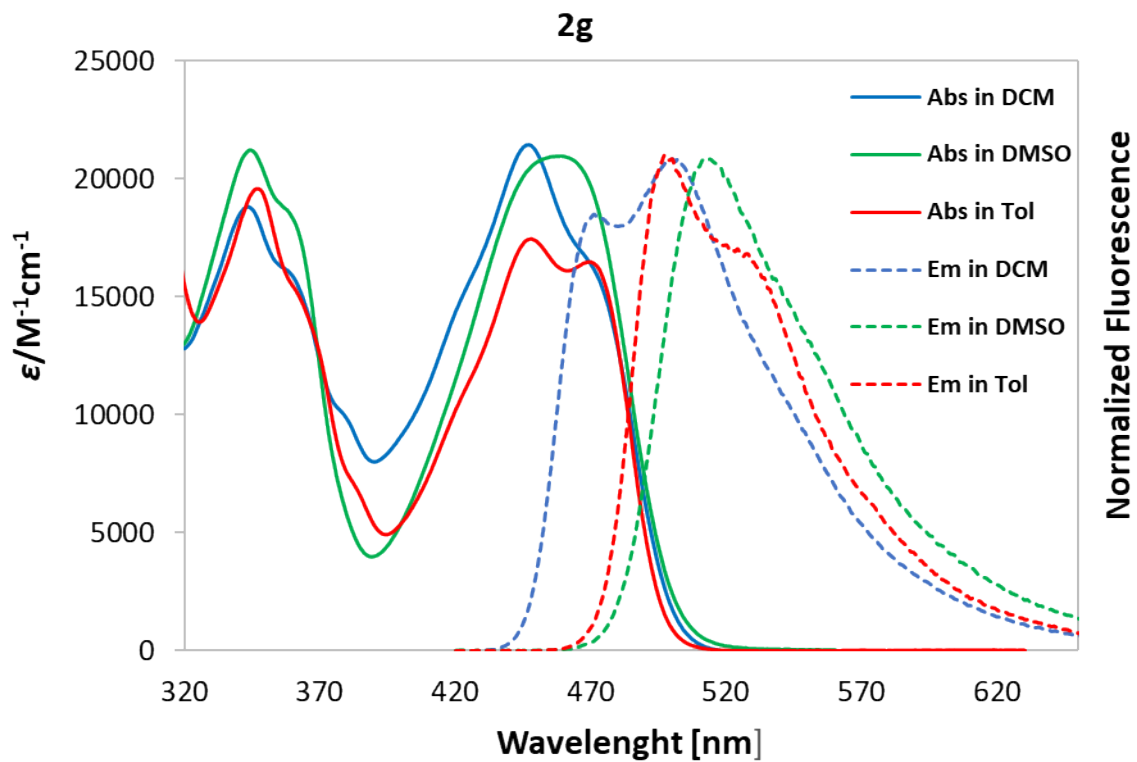
Table S5. Photophysical data of synthesized 2-oxo-pyrano[2,3-b]indolizine derivatives

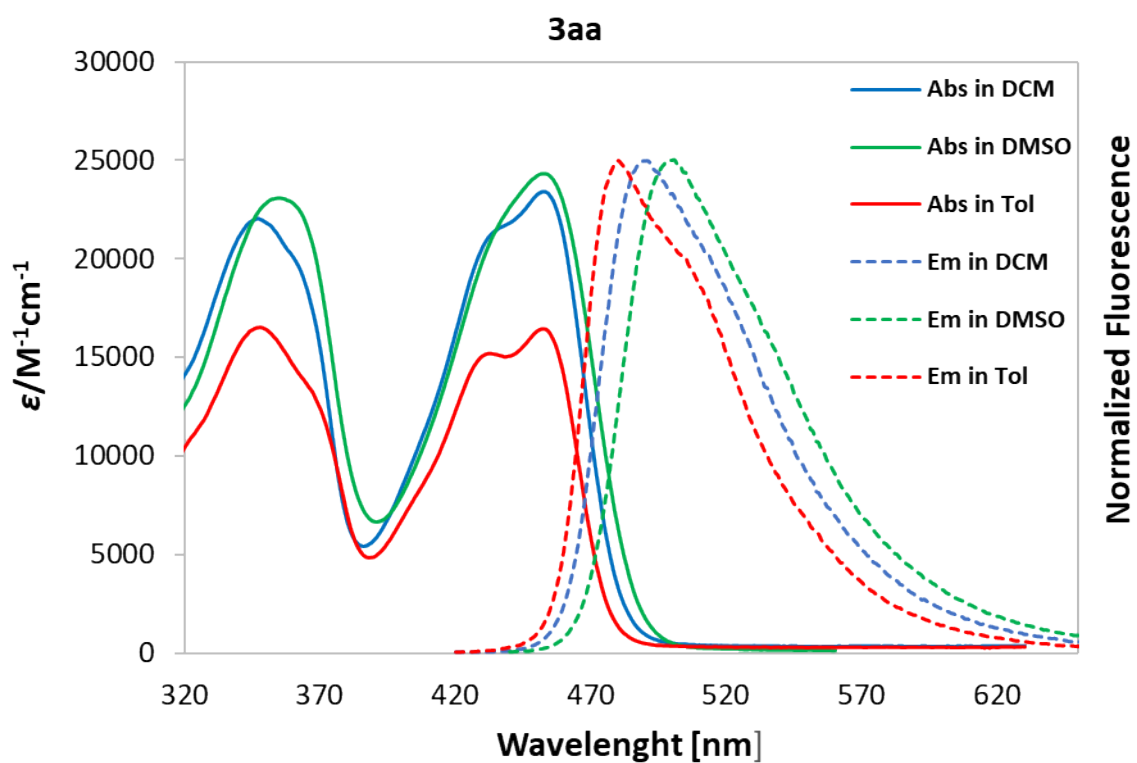
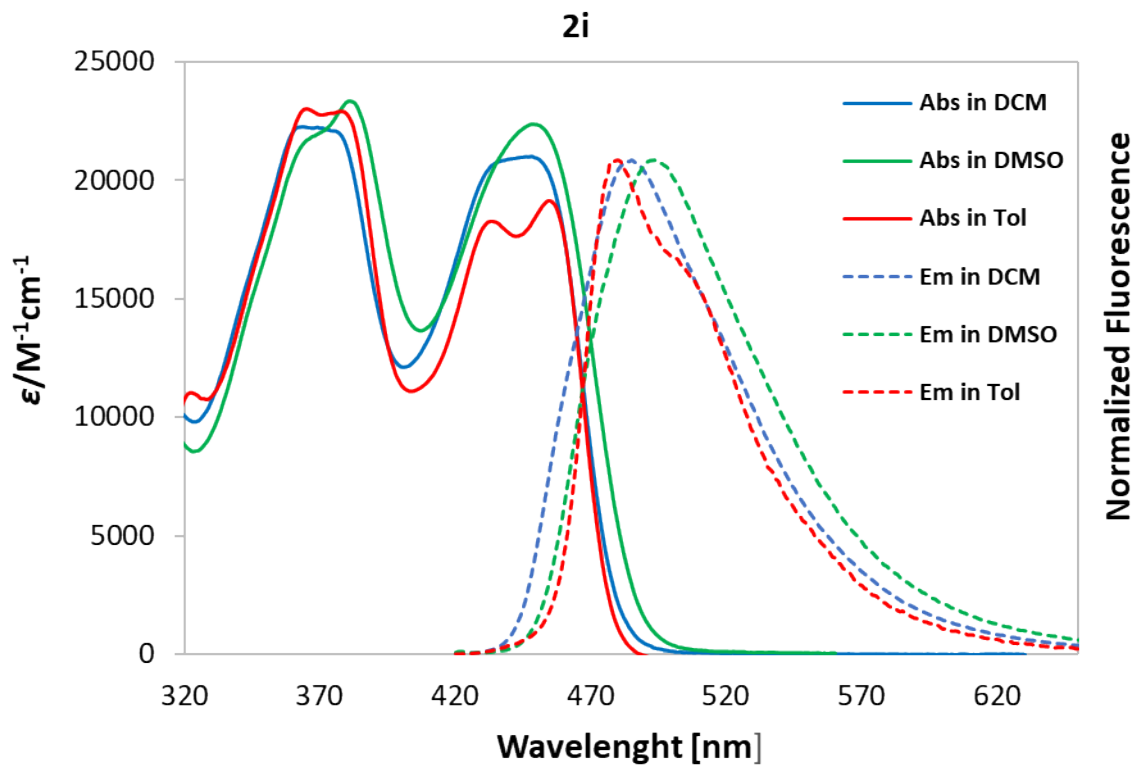
Cmp	Solv	λ_{abs} [nm]	λ_{em} [nm]	$\Delta\bar{\nu}$ [cm ⁻¹]	ϵ [M ⁻¹ cm ⁻¹]	Φ_{fl}
2a	DCM	446	464	900	30500	0,71
	DMSO	444	475	1500	33100	0,73
	Tol	441	457	800	39800	0,66
2b	DCM	449	470	1000	16300	0,77
	DMSO	449	481	1500	17600	0,76
	Tol	449	464	700	16000	0,69
2c	DCM	468	494	1100	22900	0.61
	DMSO	466	503	1600	24100	0.60
	Tol	467	486	800	20300	0.22
2d	DCM	467	499	1400	24600	0,64
	DMSO	456	507	2200	17100	0,64
	Tol	465	487	1000	8900	0,32
2e	DCM	456	470	700	39700	0,73
	DMSO	456	478	1000	36300	0,78
	Tol	457	467	500	35800	0,81
2f	DCM	436	458	1100	39700	0,33
	DMSO	437	473	1700	36300	0,35
	Tol	436	450	700	35800	0,41
2g	DCM	466	500	1500	17600	0,92
	DMSO	456	514	2500	20900	0,66
	Tol	469	500	1300	16700	0,46
2h	DCM	433	452	1000	29200	0,81
	DMSO	430	463	1700	27600	0,81
	Tol	434	449	800	23600	0,79
2i	DCM	446	485	1800	21000	0,25
	DMSO	448	493	2000	22300	0,17
	Tol	454	480	1200	19100	0,22
3aa	DCM	453	490	1700	22928	0,64
	DMSO	451	501	2200	24269	0,75
	Tol	452	480	1300	16484	0,58
3ab	DCM	452	491/642	6500	27700	0.03
	DMSO	448	492/702	8100	20000	<0.01
	Tol	452	477	1200	30100	0.34
3ac	DCM	457	514	2400	19600	0,65
	DMSO	457	521	2700	19300	0,60
	Tol	454	501	2100	17000	0,58
4a	DCM	426	448	1200	31800	0,77
	DMSO	426	447	1100	30400	0,78
	Tol	428	444	800	28600	0,70
6a^b	DCM	509	575	2300	24400	0.44
	DMSO	490	594	3200	20400	0.37

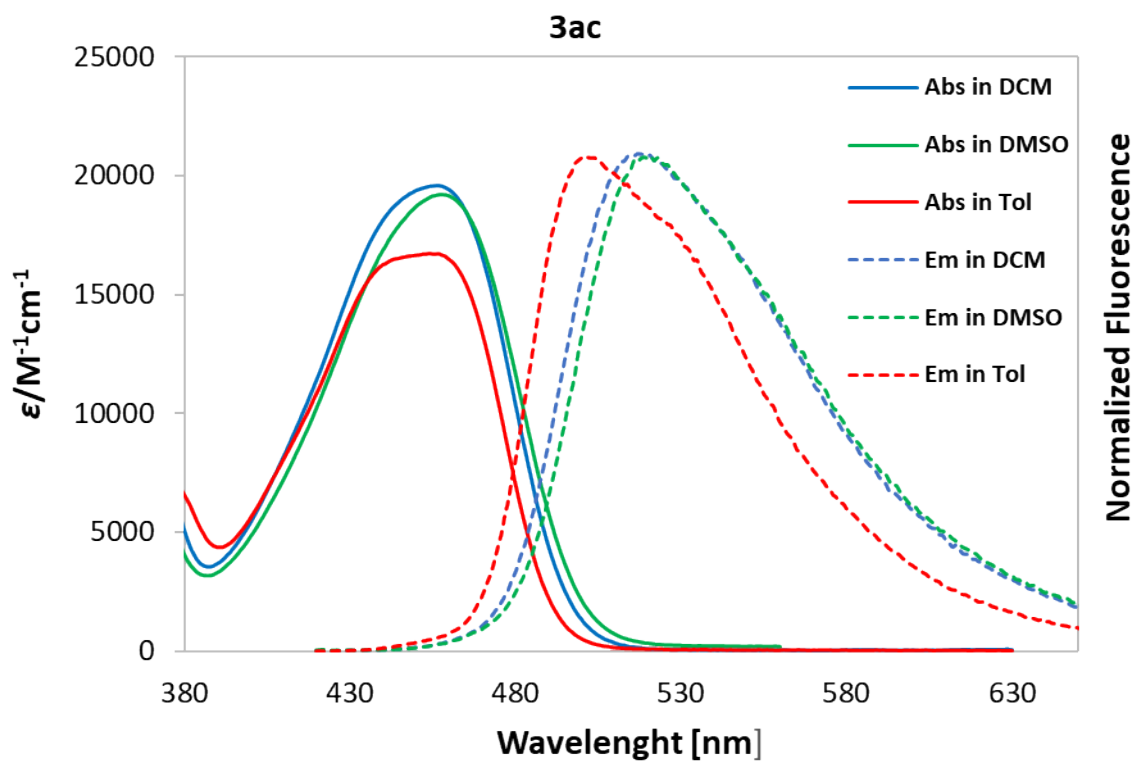
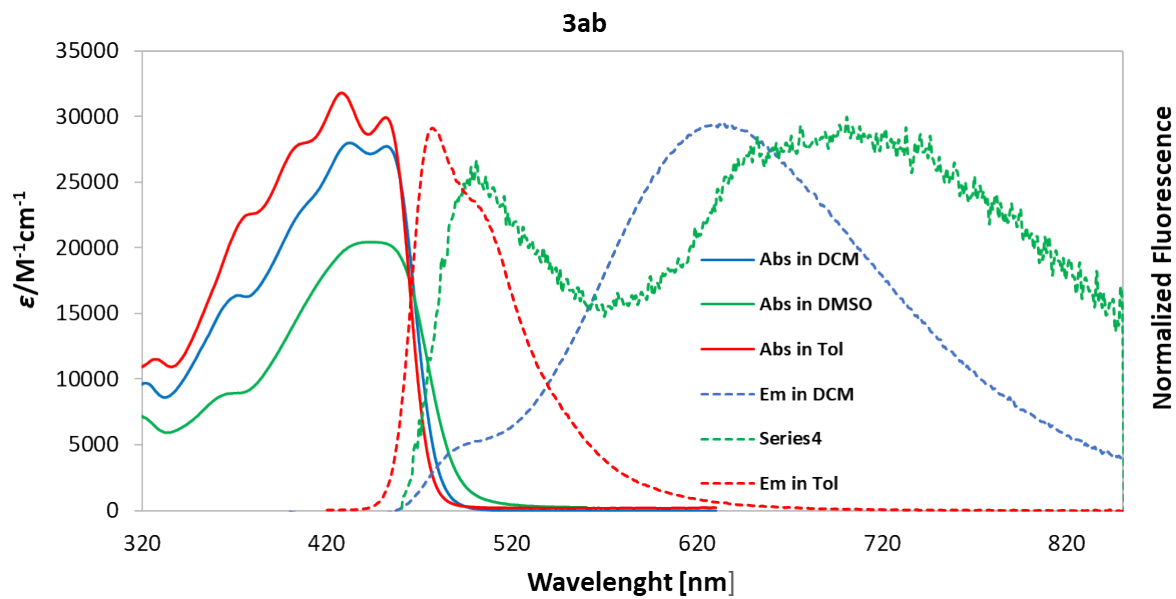












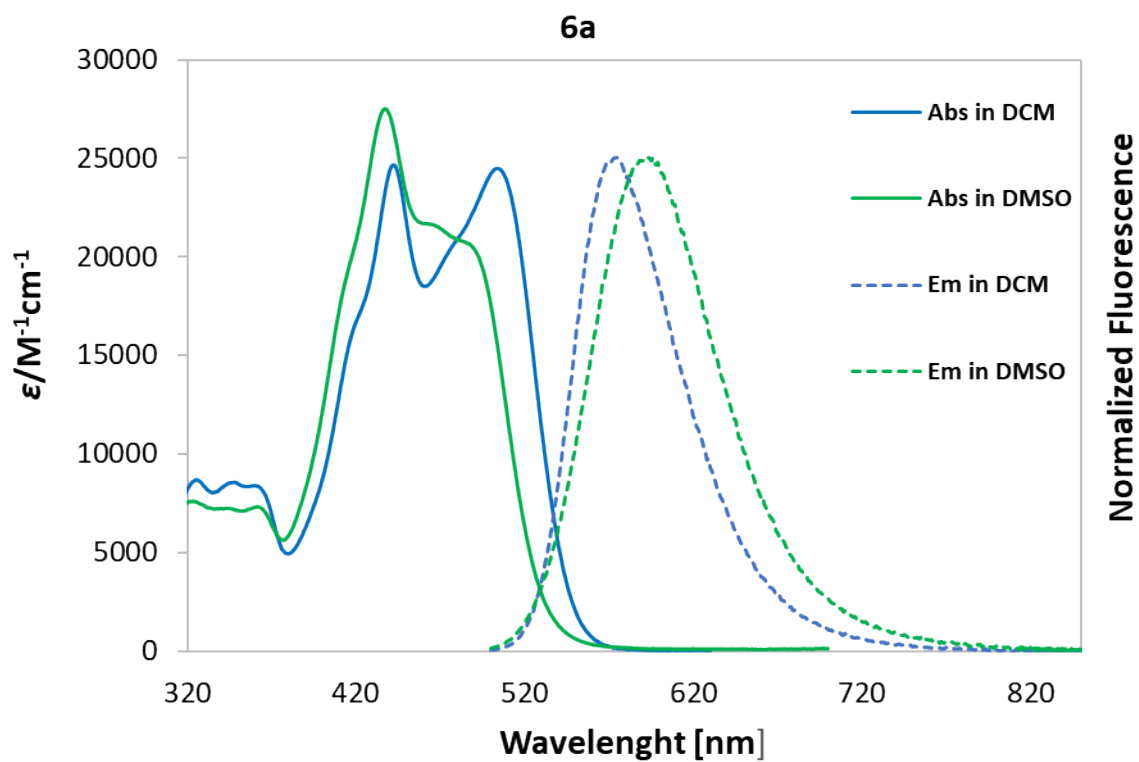
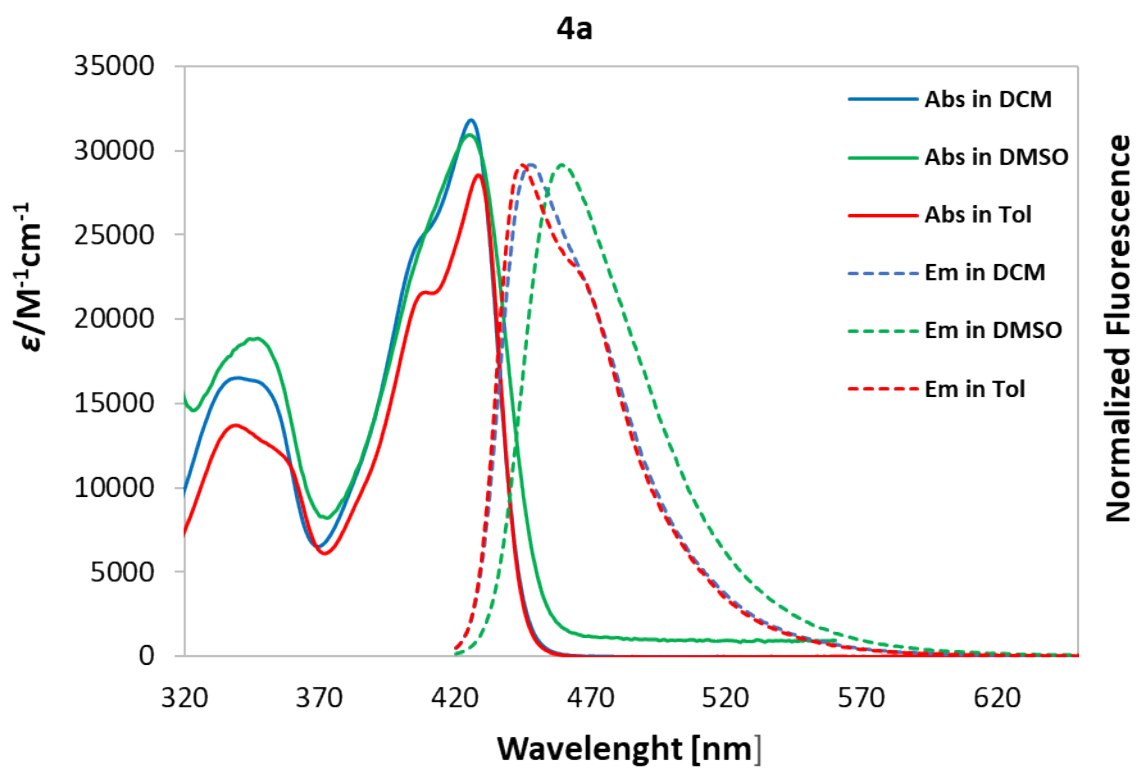


Figure S10. Absorption (solid) and fluorescence spectra (dashed lines) of compounds in solvents.

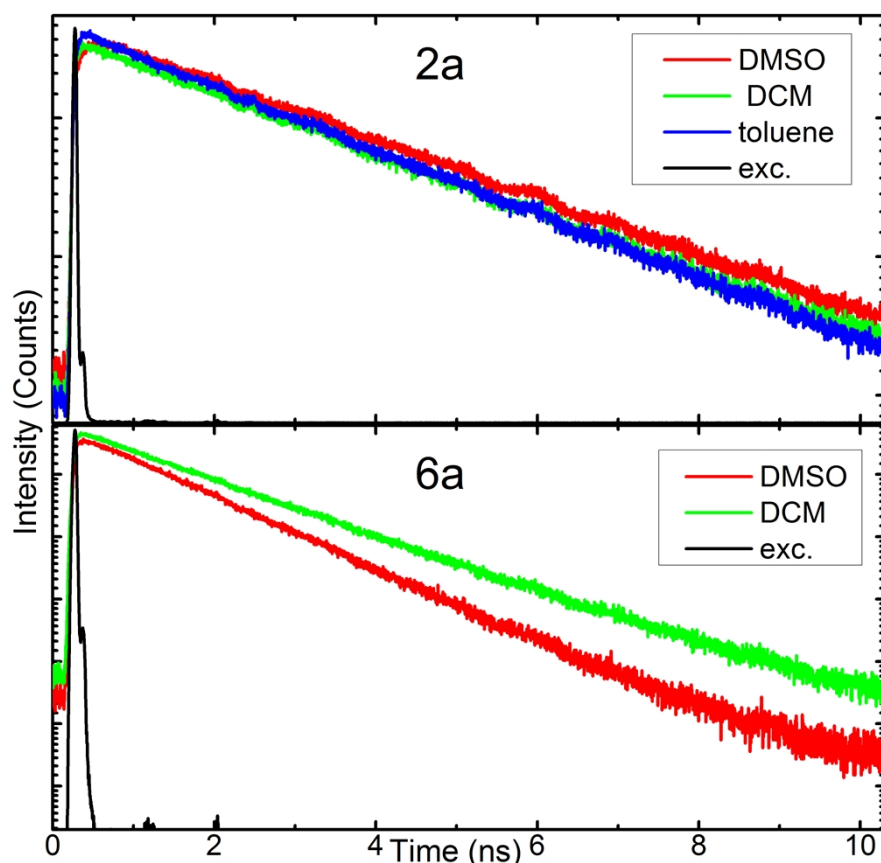


Figure S11. Semi logarithmic plot of fluorescence decay traces of **2a** (upper) and **6a** (bottom panel) in solvents. Decay curves recorded with resolution of 3.05 ps per channel at 20°C. Excitation at 387.5 nm.

Table S6. Fluorescence decay time τ determined from decay profiles presented in Figure S11, quantum yield Φ (copied from Table S5), radiative k_r and non-radiative k_{nr} rate constants as well as fluorescence excitation and observation wavelengths for **2a** and **6a** in solvents. $k_r = \Phi/\tau$ and $k_{nr} = 1/\tau - k_r$.

Compound	Solvent	Exc./nm	Obs./nm	τ / ns	Φ	$k_r / 10^9 \text{ s}^{-1}$	$k_{nr} / 10^9 \text{ s}^{-1}$
2a	Toluene	387.5	470	3.61	0.66	0.127	0.15
2a	DCM	387.5	467	3.52	0.71	0.139	0.14
2a	DMSO	387.5	467	3.86	0.73	0.132	0.13
6a	DCM	387.5	578	2.1	0.44	0.21	0.27
6a	DMSO	387.5	591	1.66	0.37	0.22	0.38

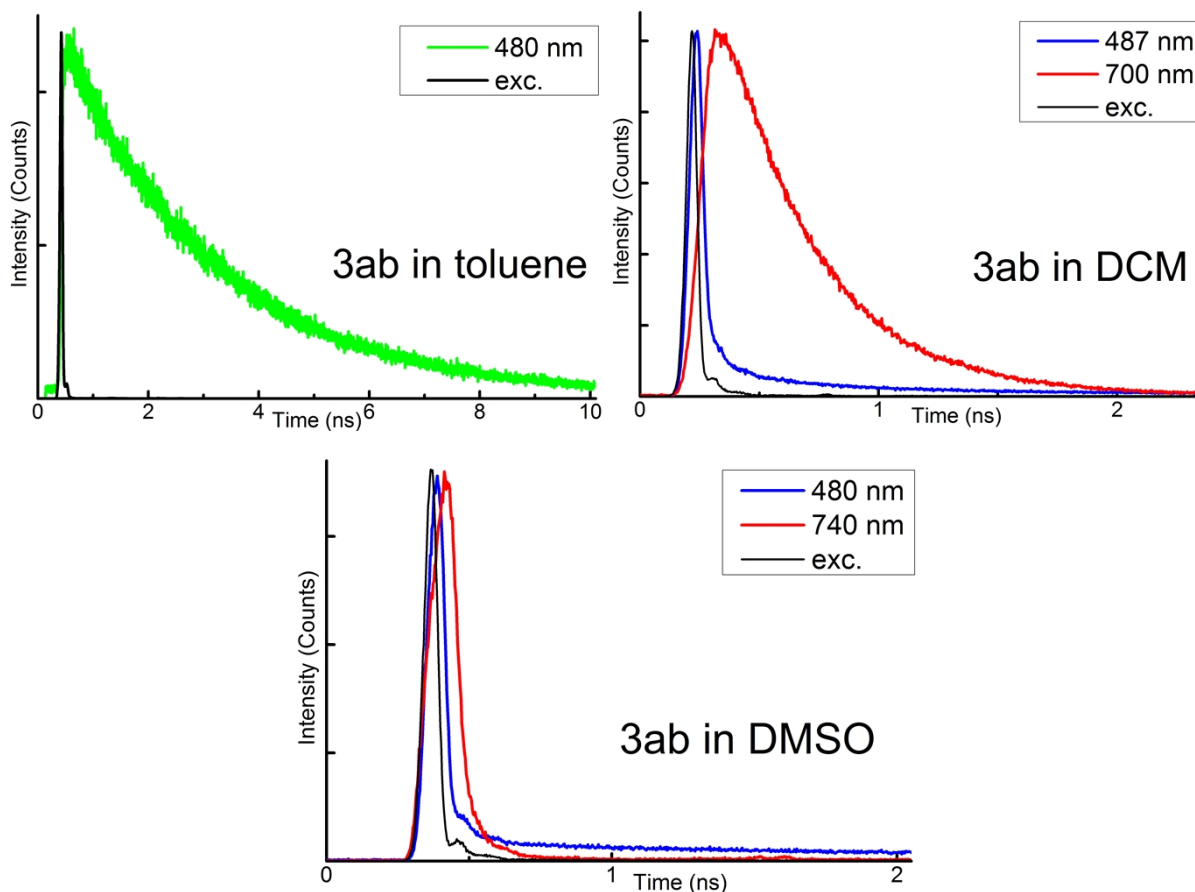


Figure S12. Plot of fluorescence decay traces of **3ab** in solvents: toluene (upper), dichloromethane (middle) and DMSO (bottom panel). Decay curves recorded with resolution of 3.05 ps per channel at temperature 20°C. Excitation at 387.5 nm. Legends specify wavelength of observation and color of traces.

Table S7. Fluorescence decay times, τ , and amplitudes, A , obtained from decay profiles presented in Figure S12, Excitation at 387.5 nm. Radiative k_r and non-radiative k_{nr} rate constants are calculated for single – exponential decay in toluene only.

Compound	Solvent	Obs./nm	τ_1 / ns	τ_2 / ns	A_1	A_2	Φ	$k_r / 10^9 \text{ s}^{-1}$	$k_{nr} / 10^9 \text{ s}^{-1}$
3ab	Toluene	480	2.62				0.34	0.088	0.29
3ab	DCM	487	0.02	0.356	70.9	1.414			
3ab	DCM	700	0.055	0.356	-15	18.7			
3ab	DMSO	480	0.015	2.22	86	0.63			
3ab	DMSO	740	0.055						

3. Imaging Studies

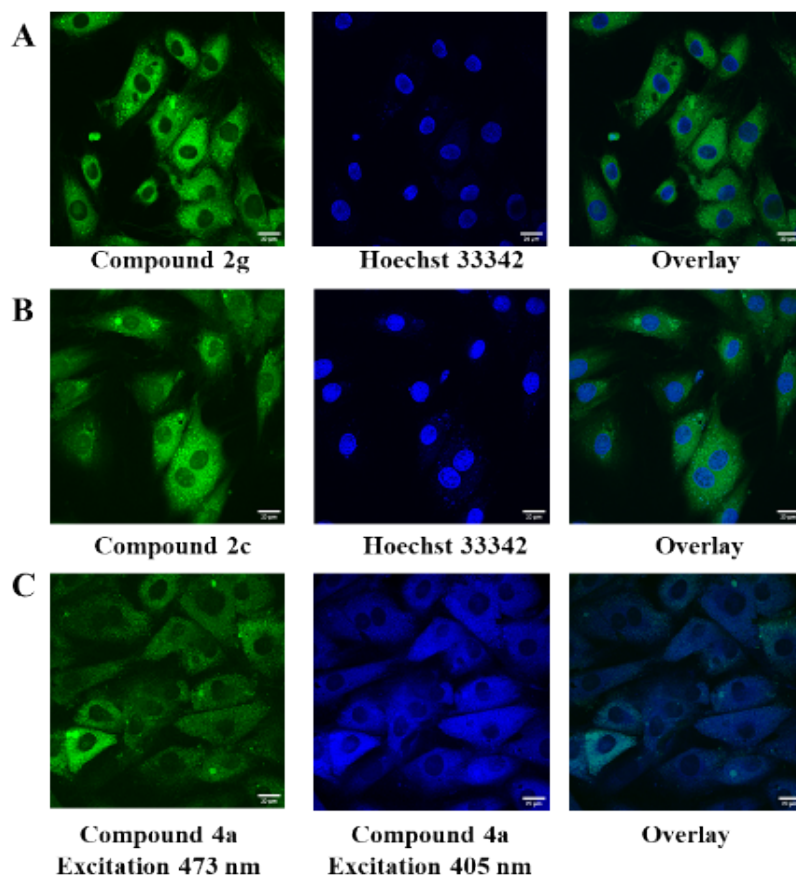
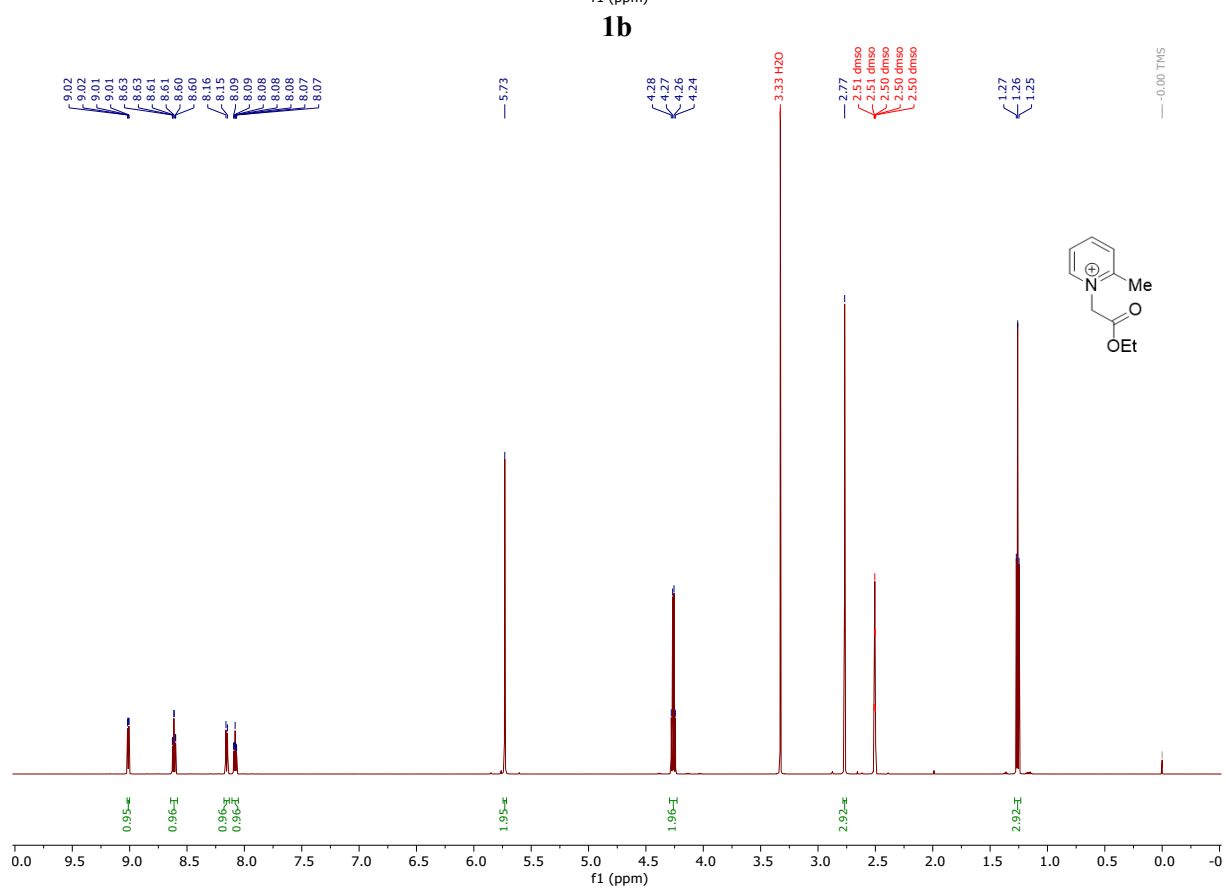
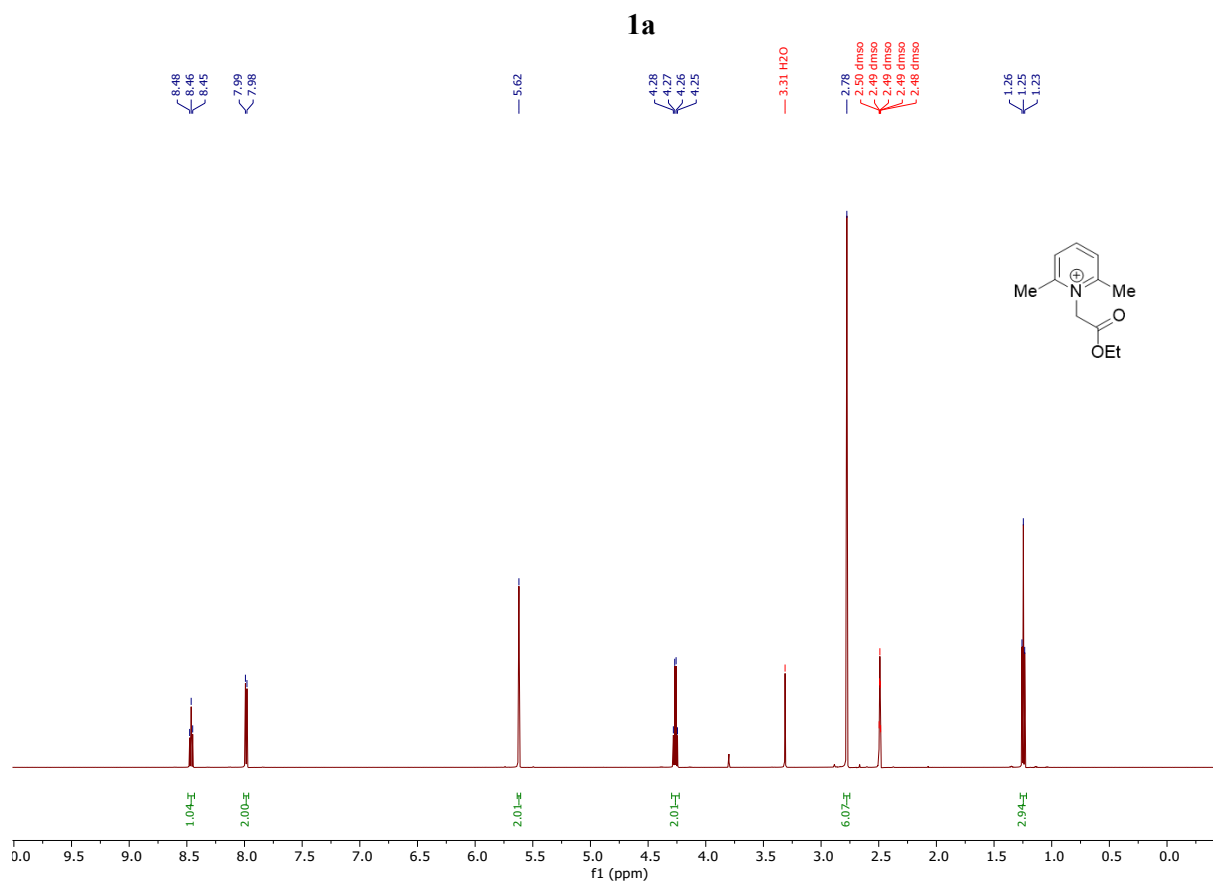
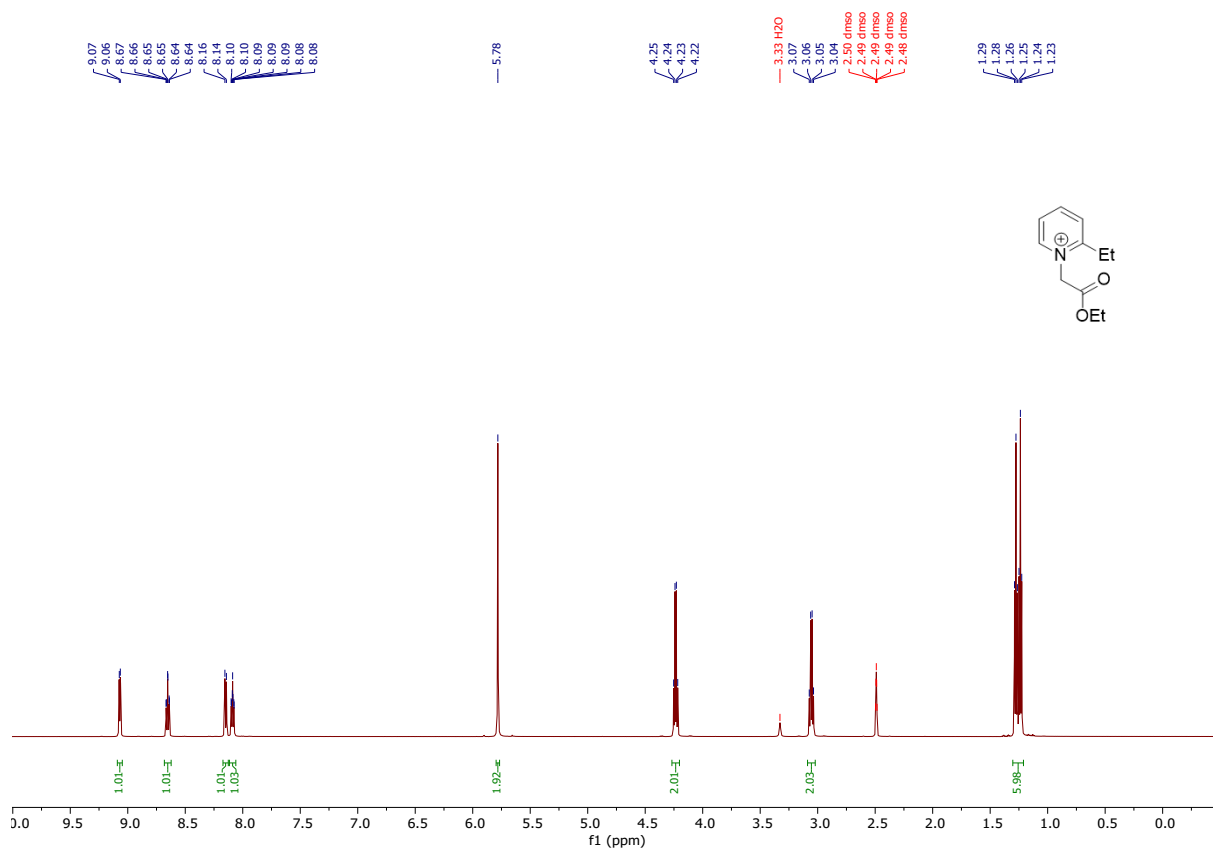


Figure S13. Intracellular localization of compound **2g**, **2c** and **4a** in H9c2 cells detected using confocal fluorescence microscopy. A) Intracellular localization of **2g** compound in relation to Hoechst 33342. B) Intracellular localization of **2c** compound in relation to Hoechst 33342. C) Intracellular localization of **4a** compound in two excitation wavelength and its Overlay.

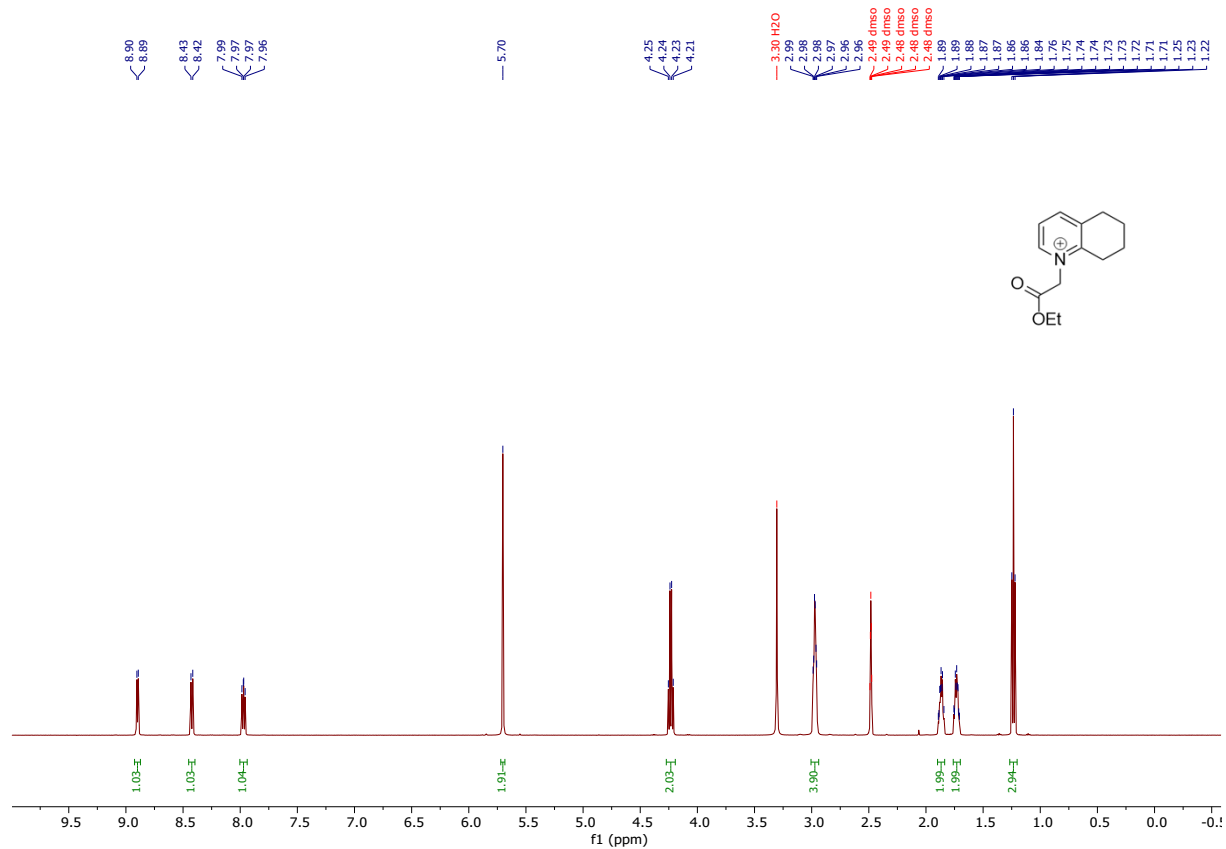
4. ¹H NMR and ¹³C NMR spectra of new compounds



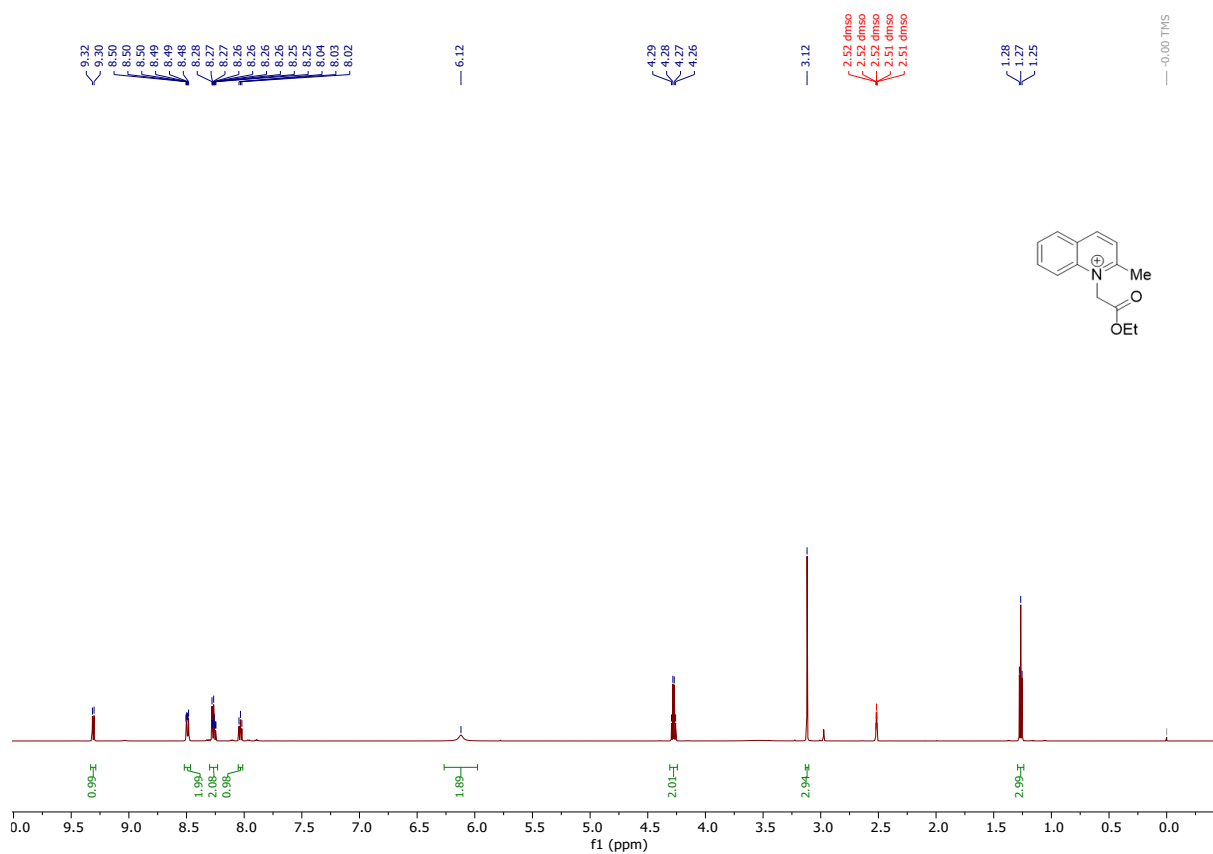
1c



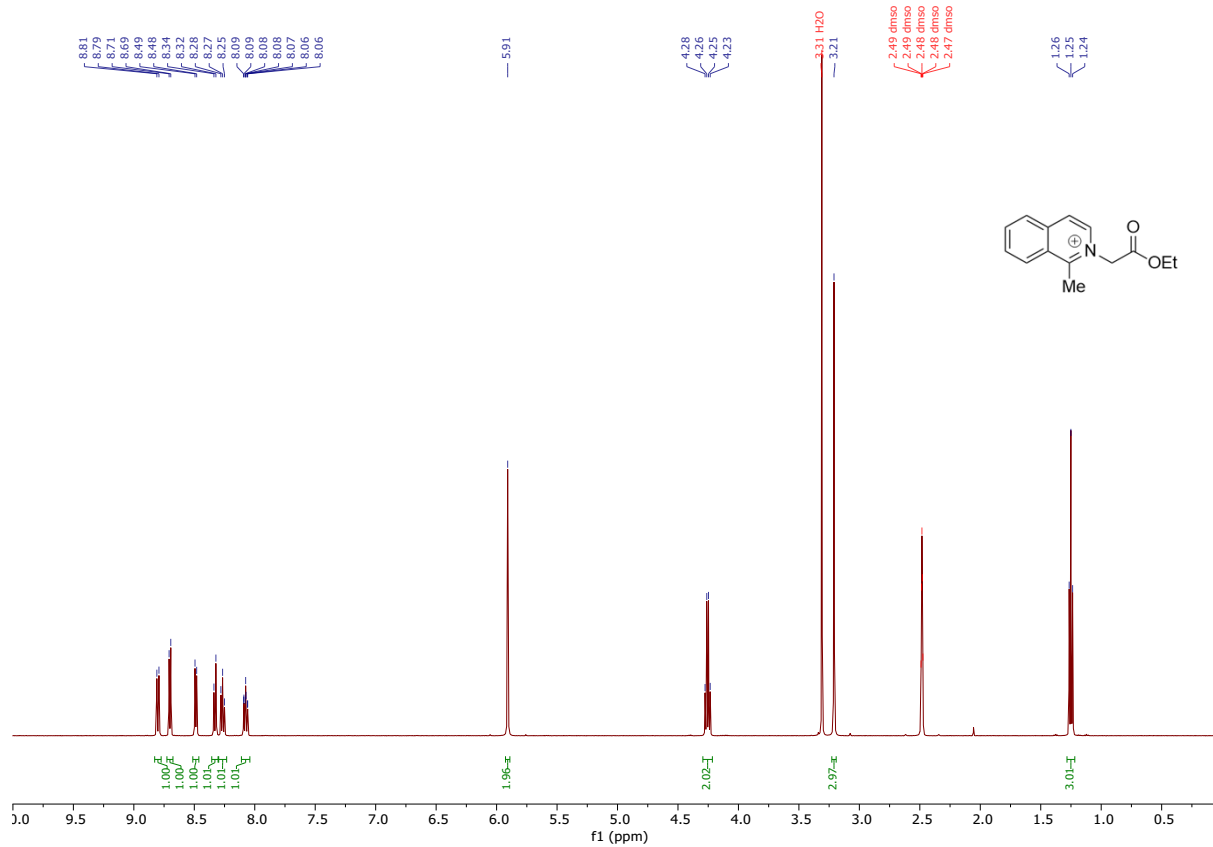
1d

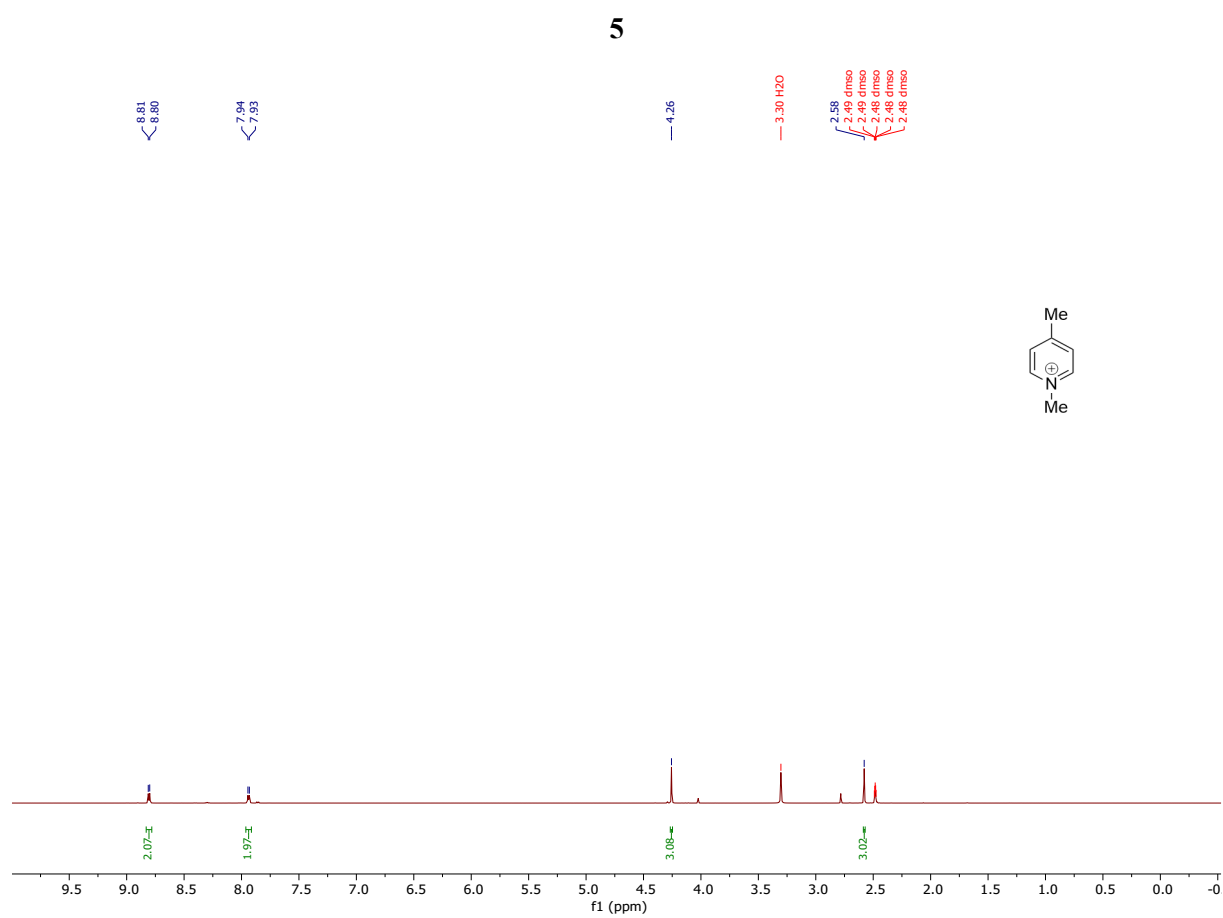
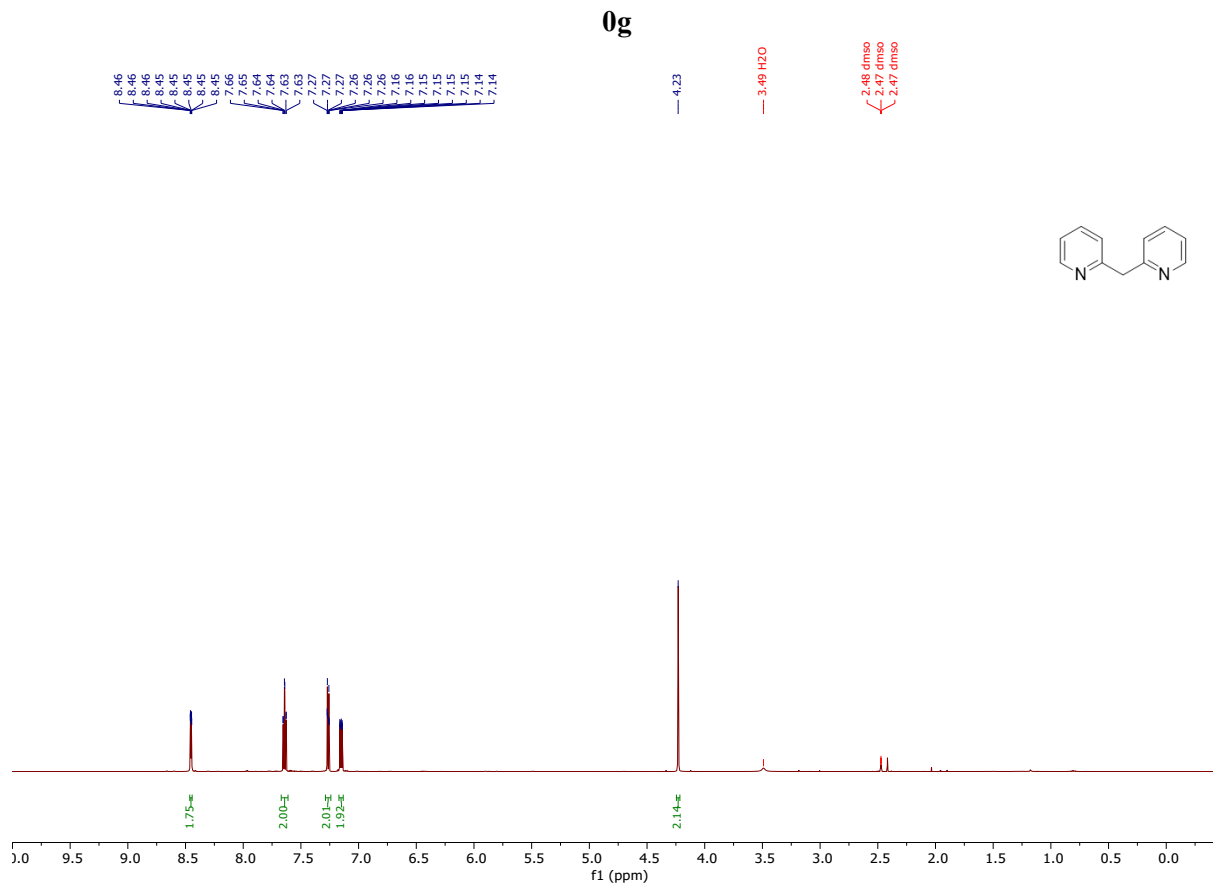


1e

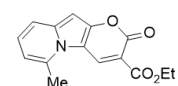
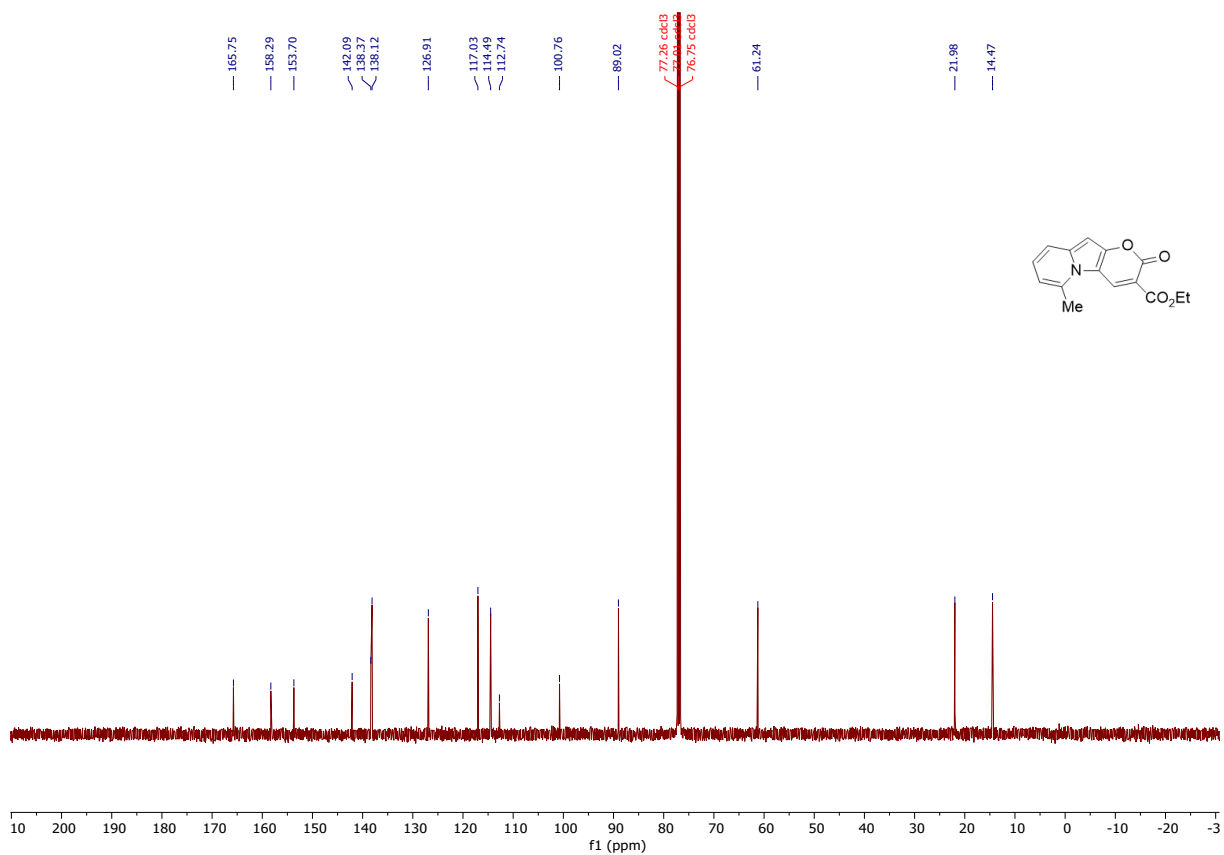
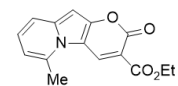
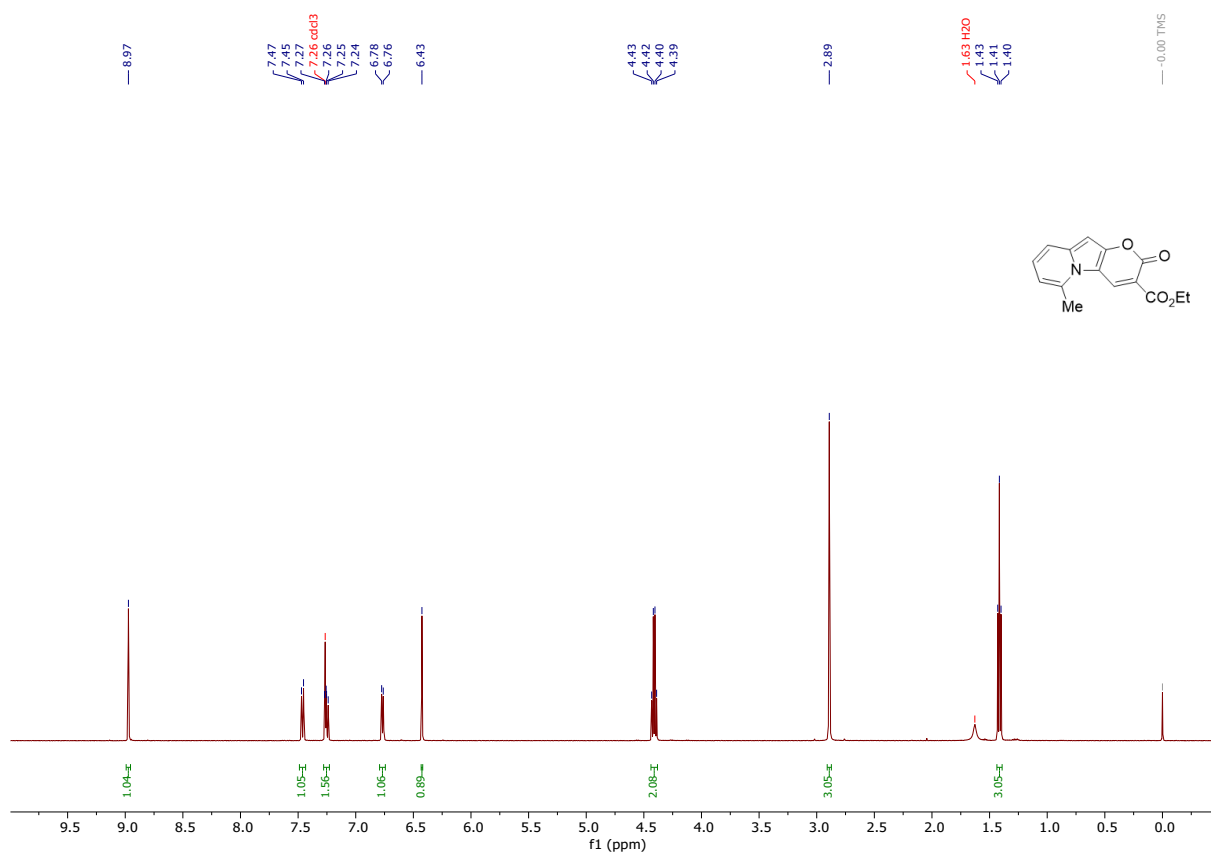


1f

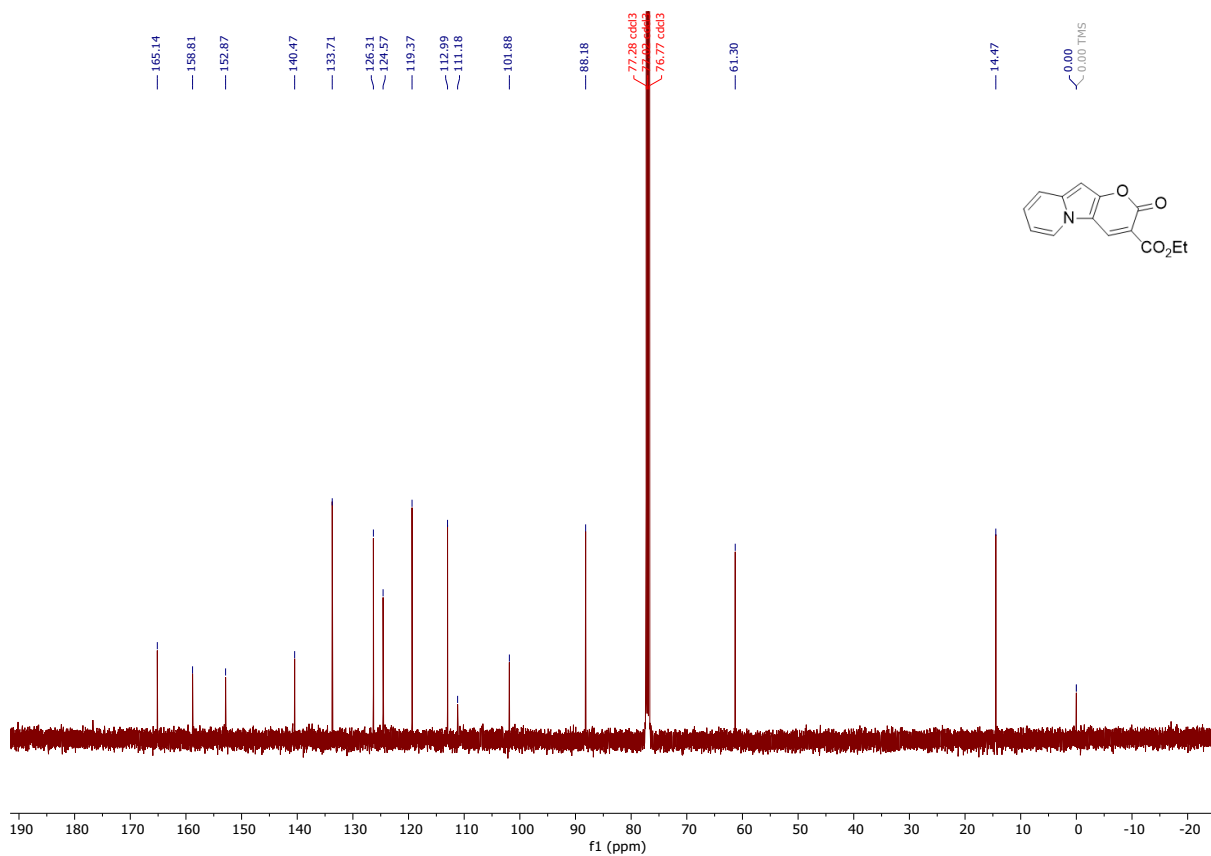
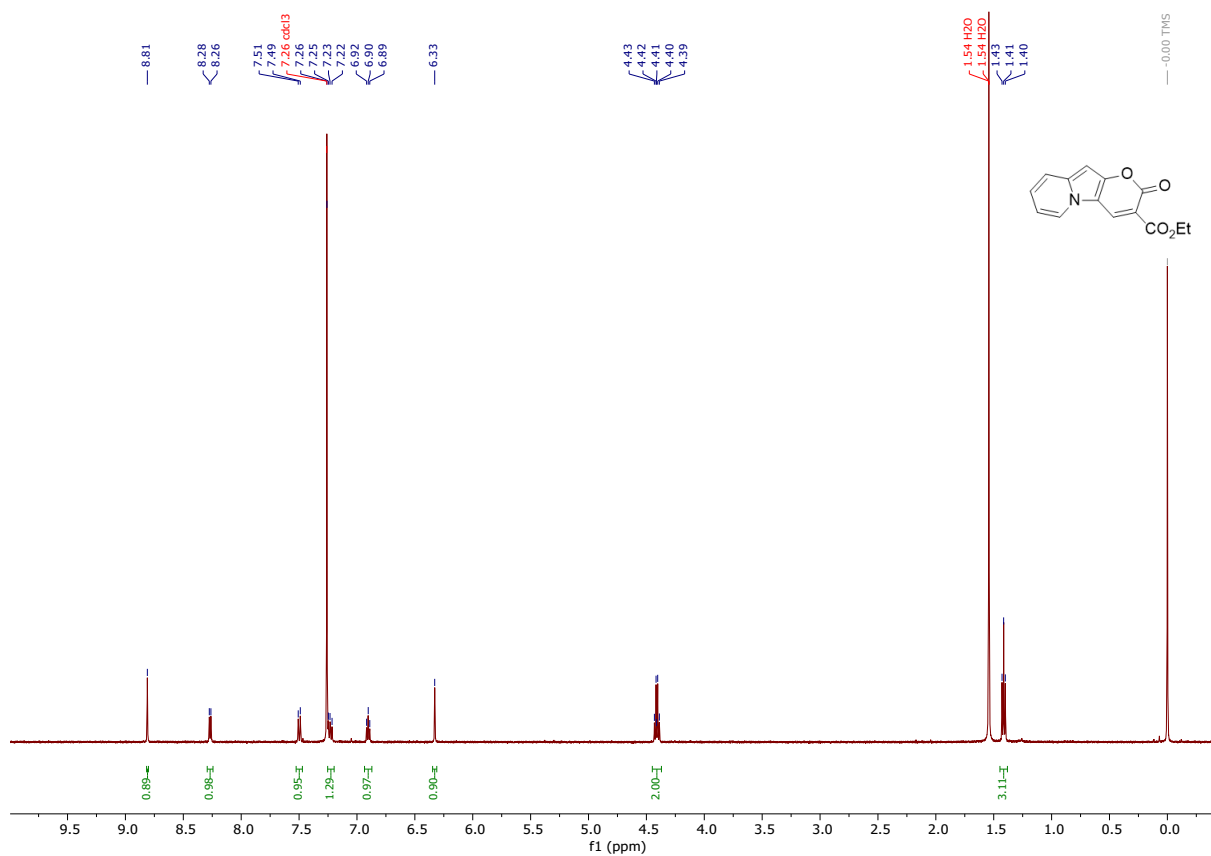




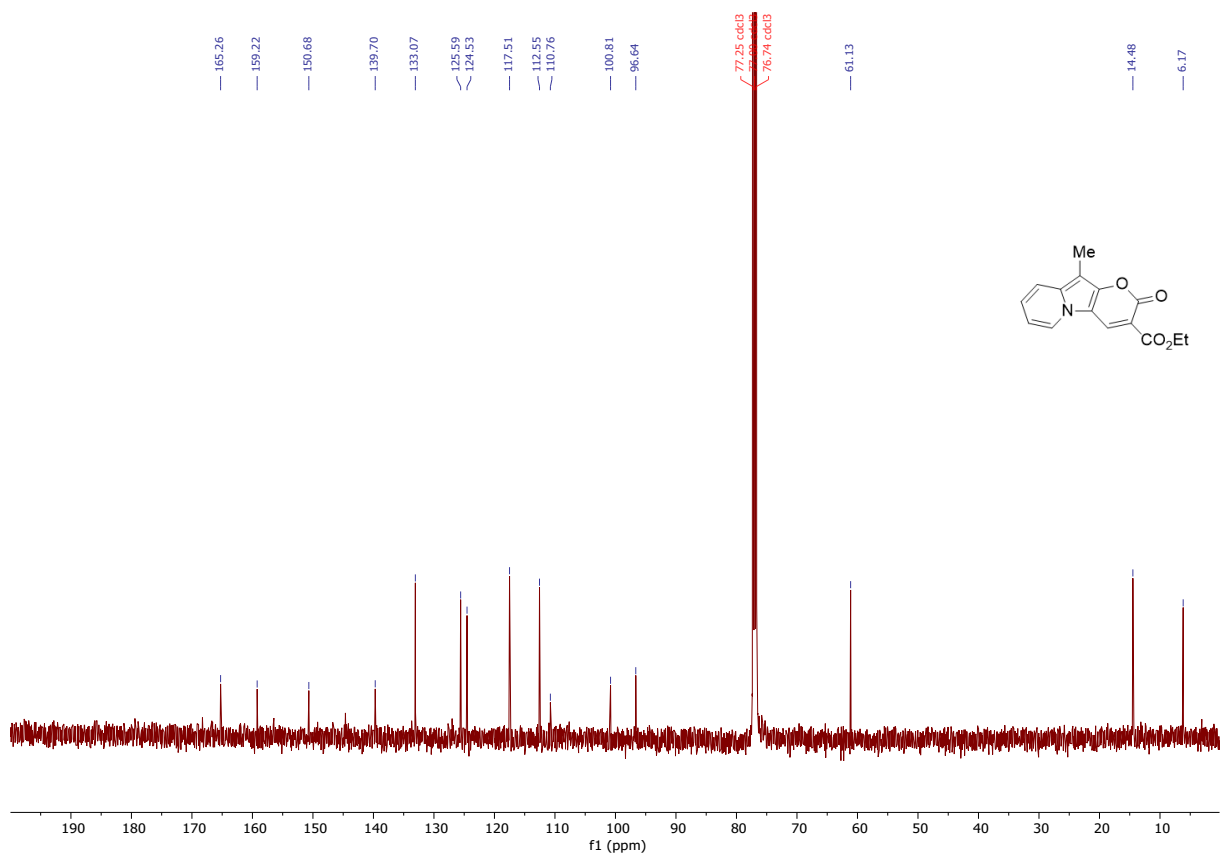
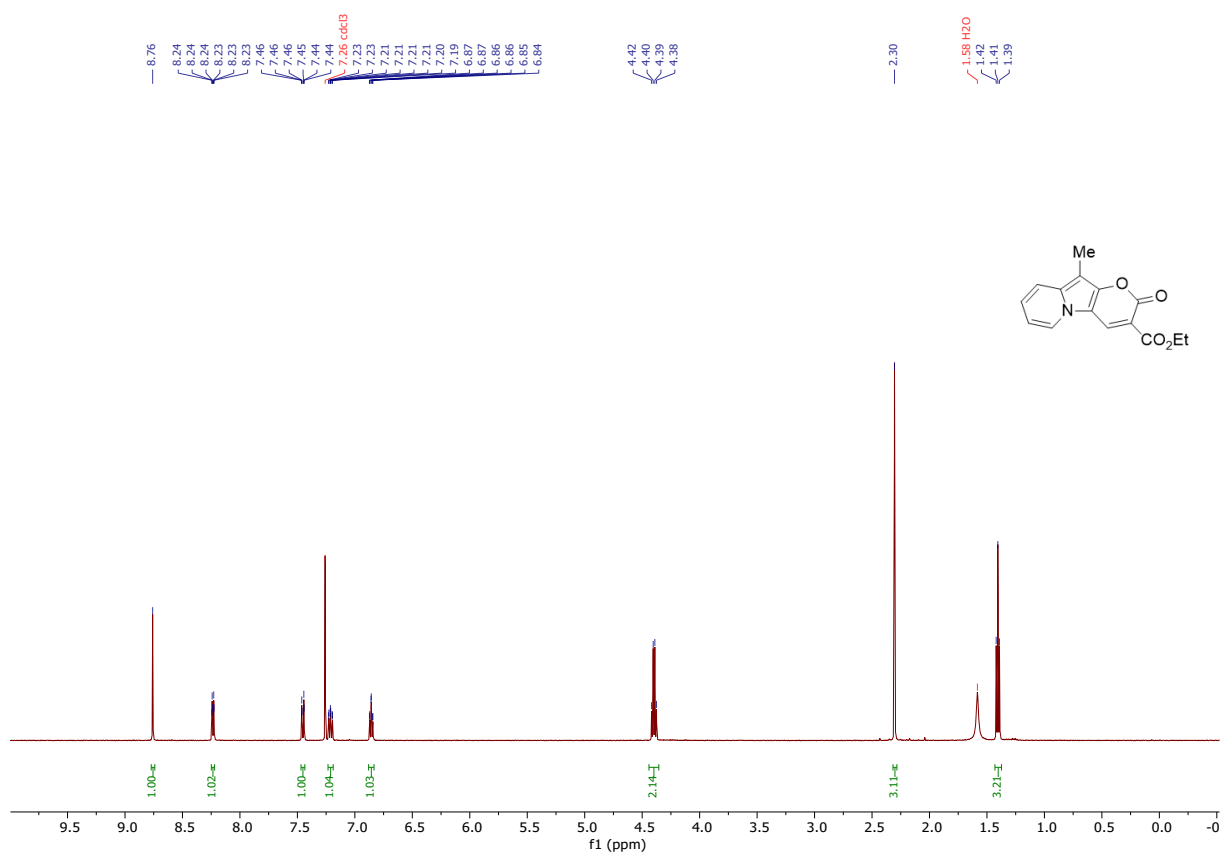
2a



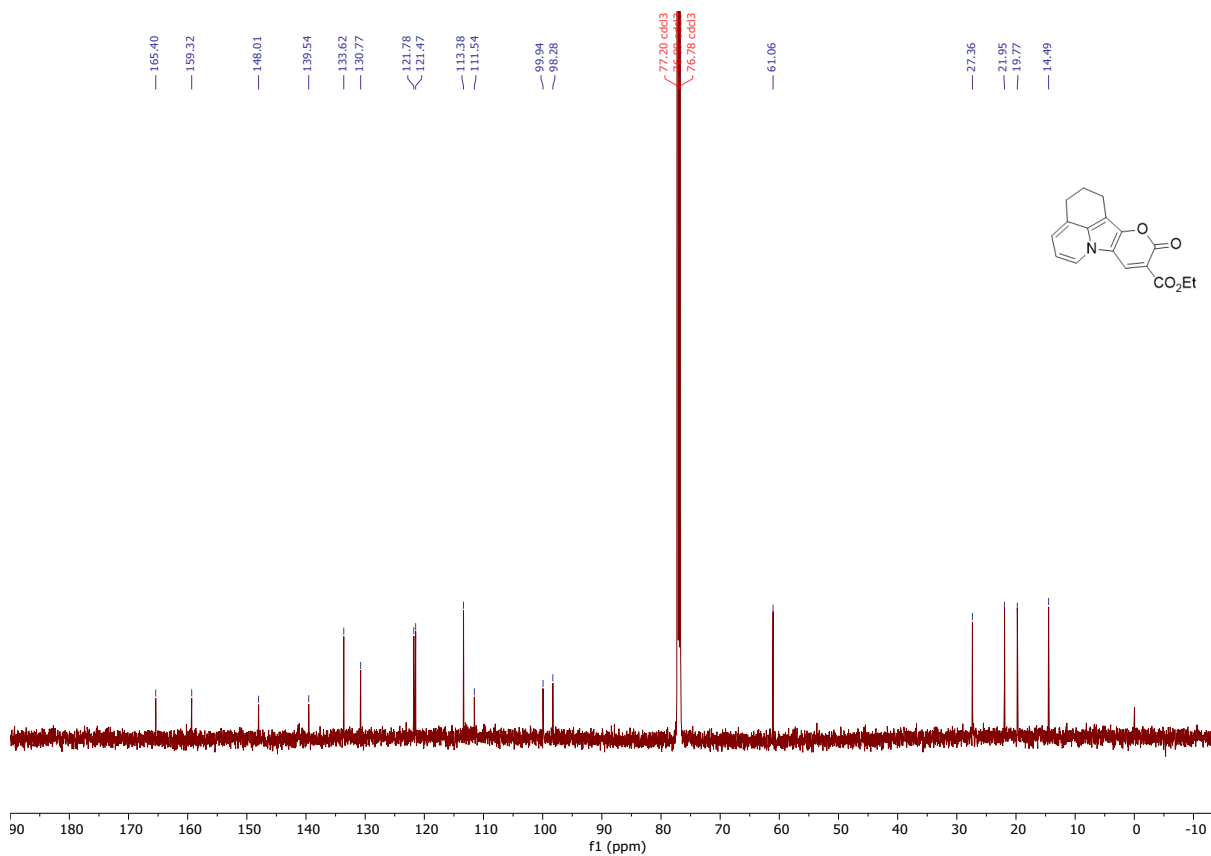
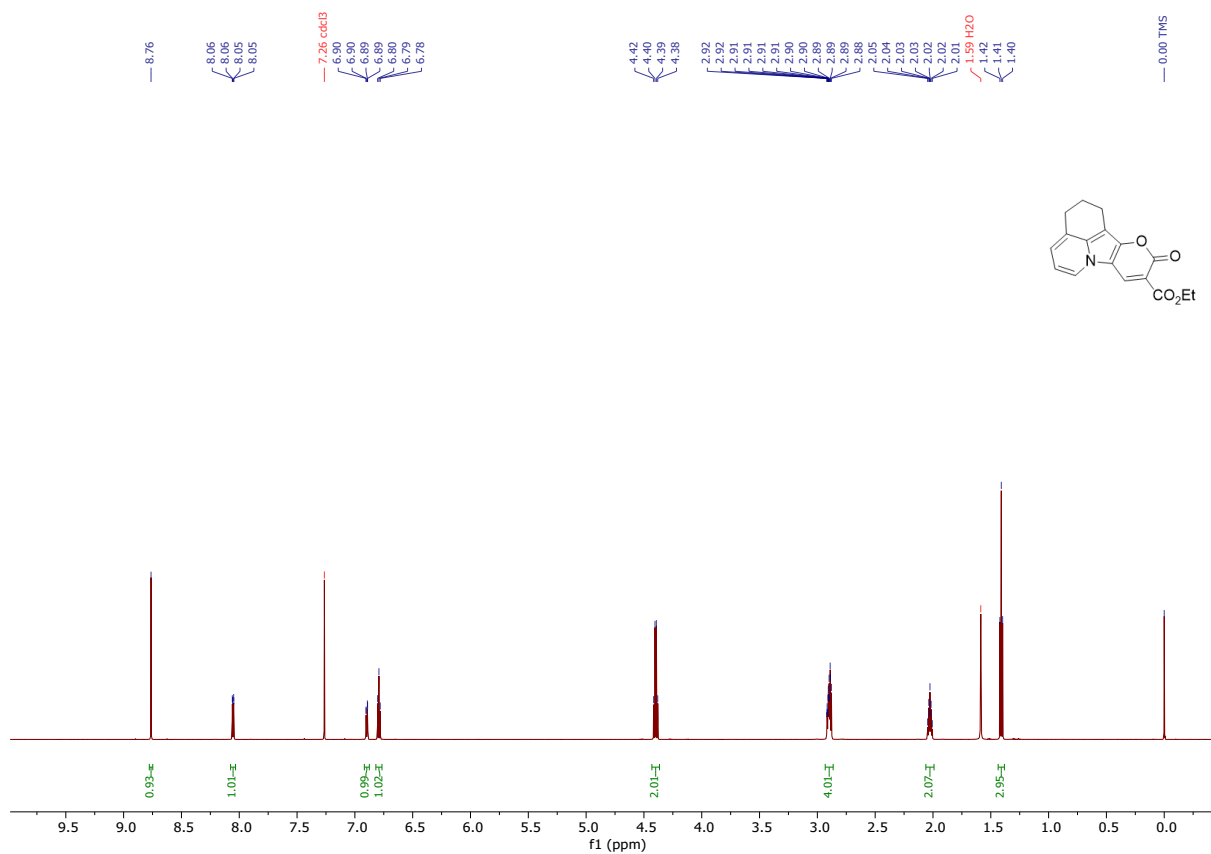
2b



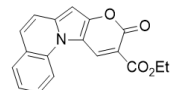
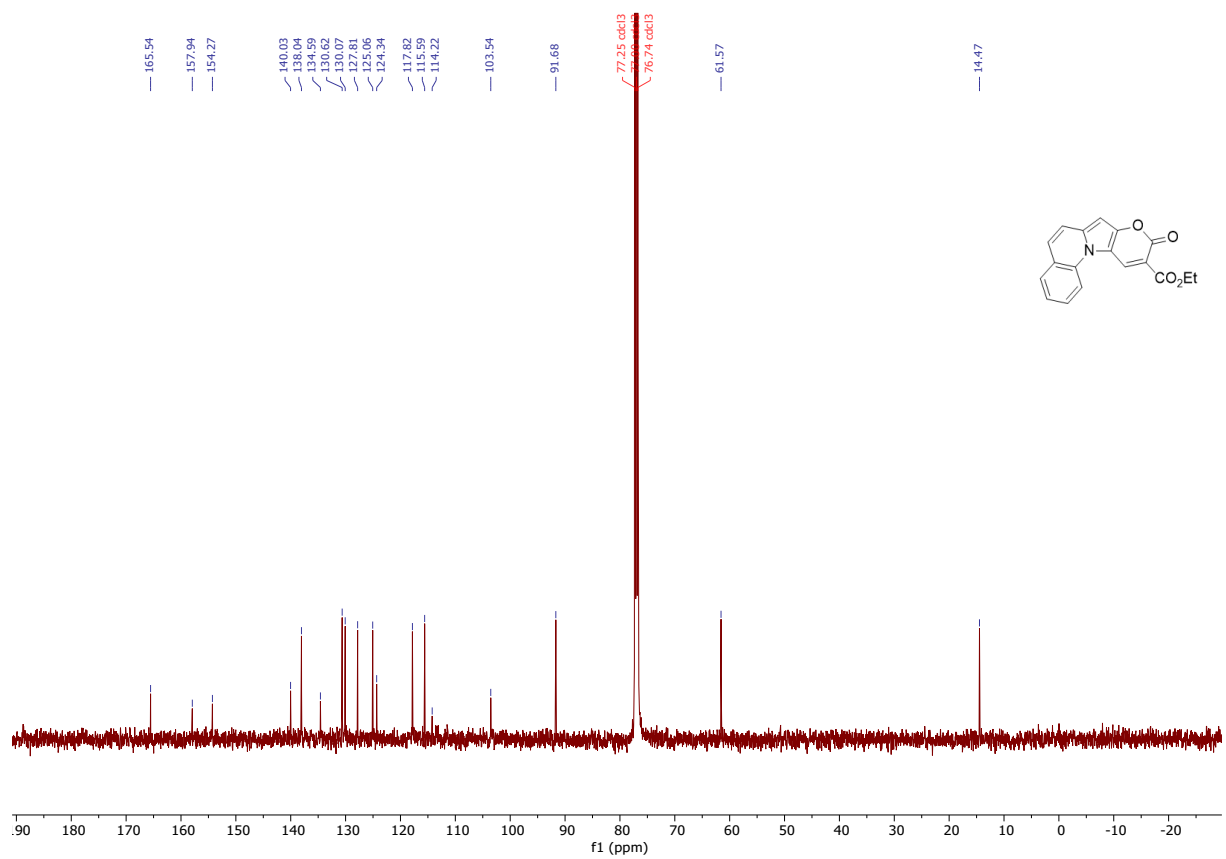
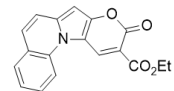
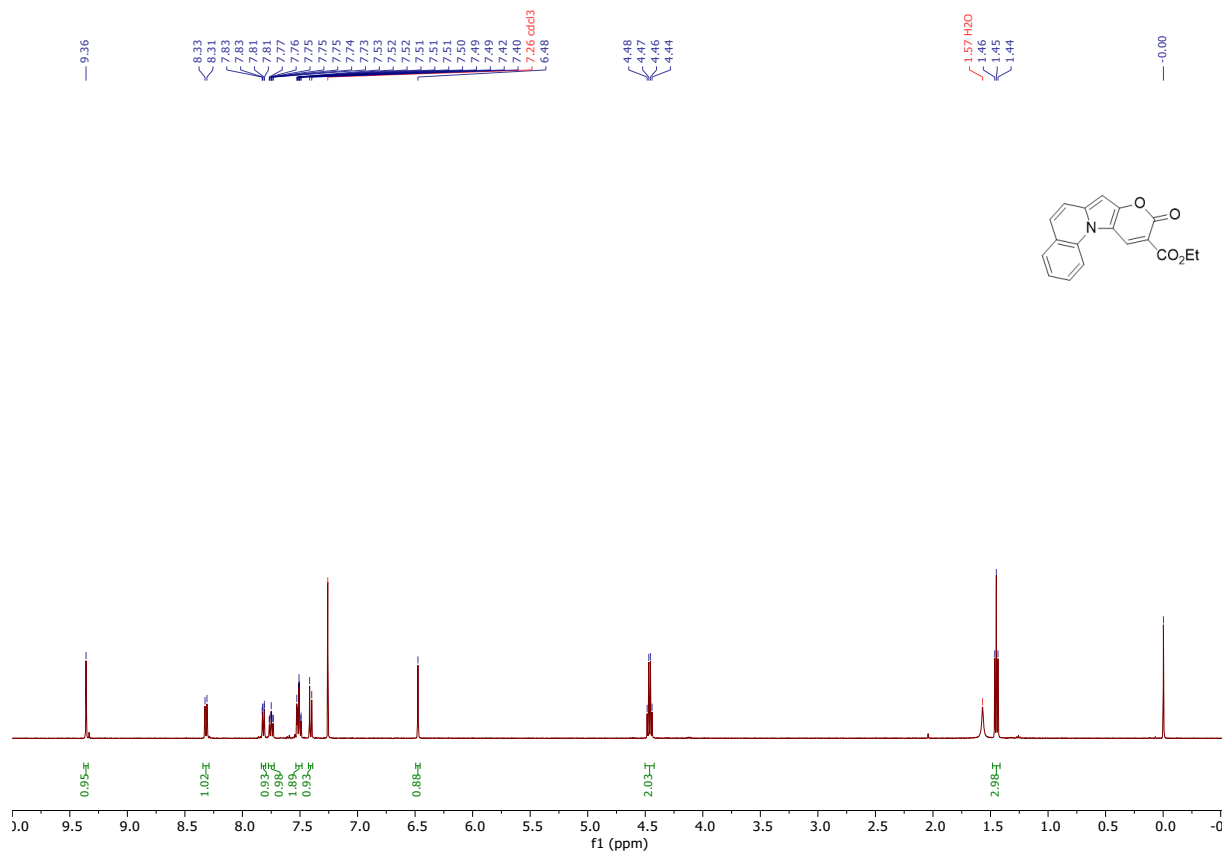
2c



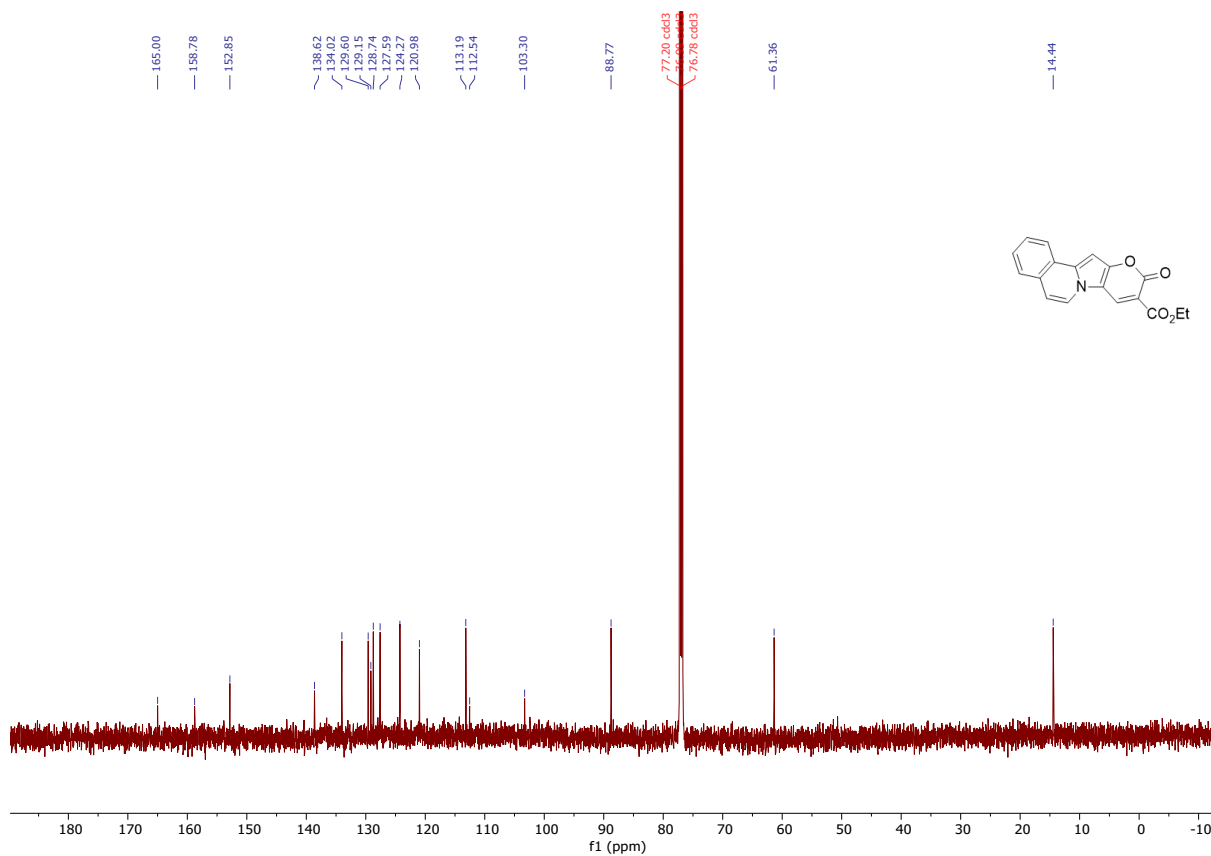
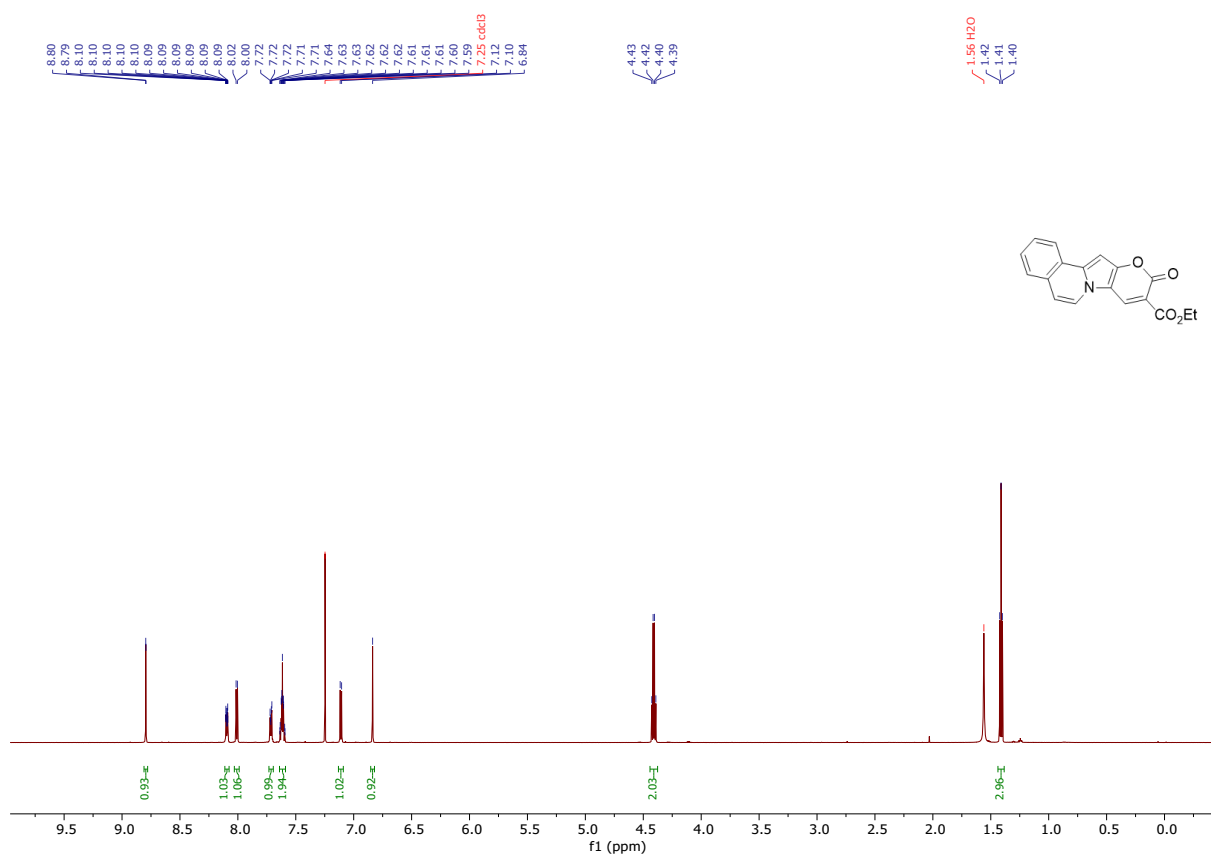
2d



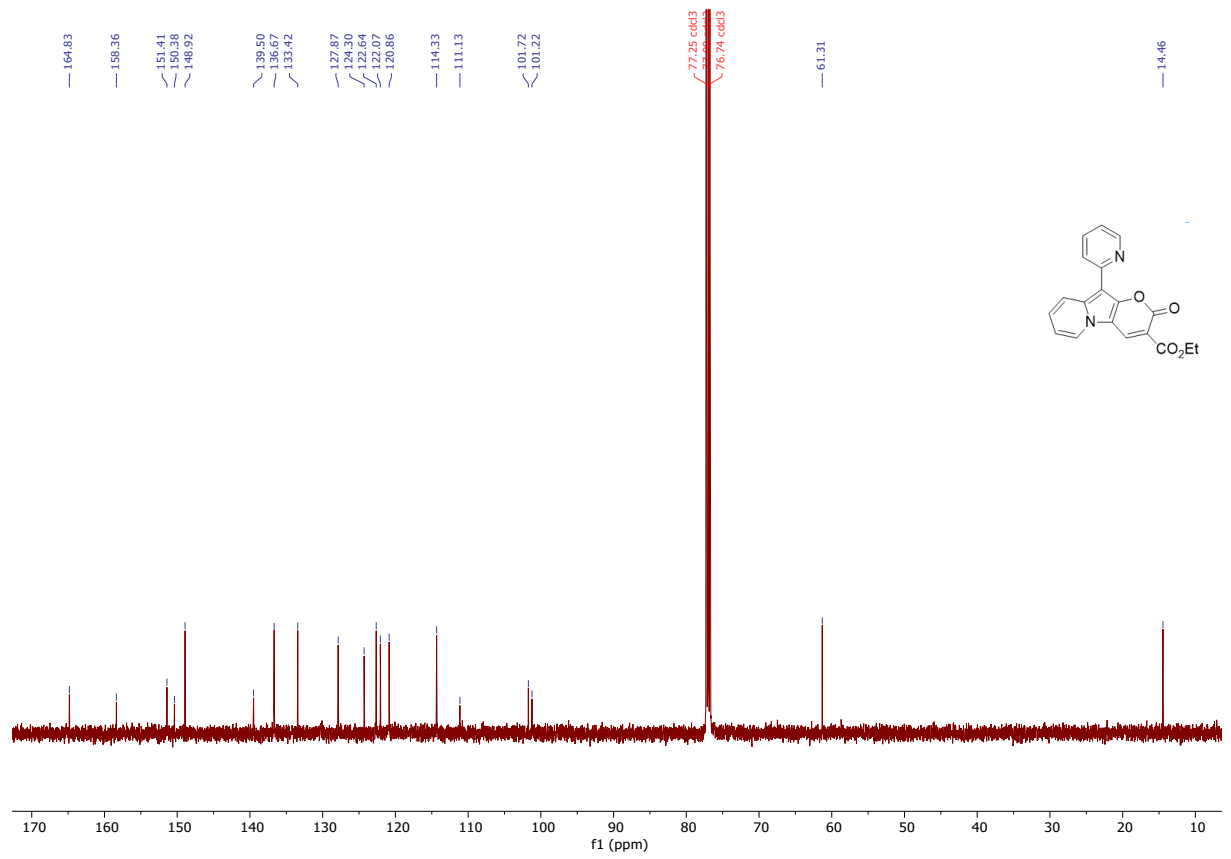
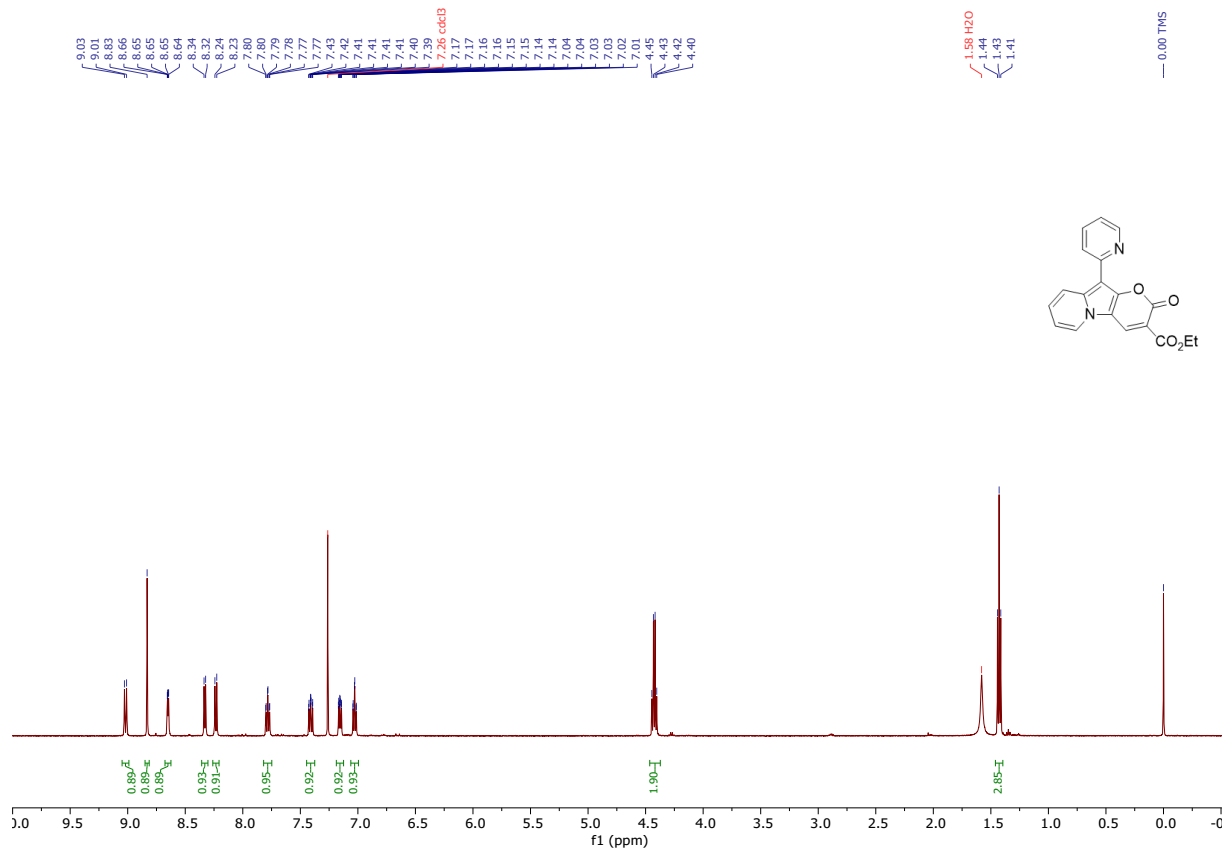
2e



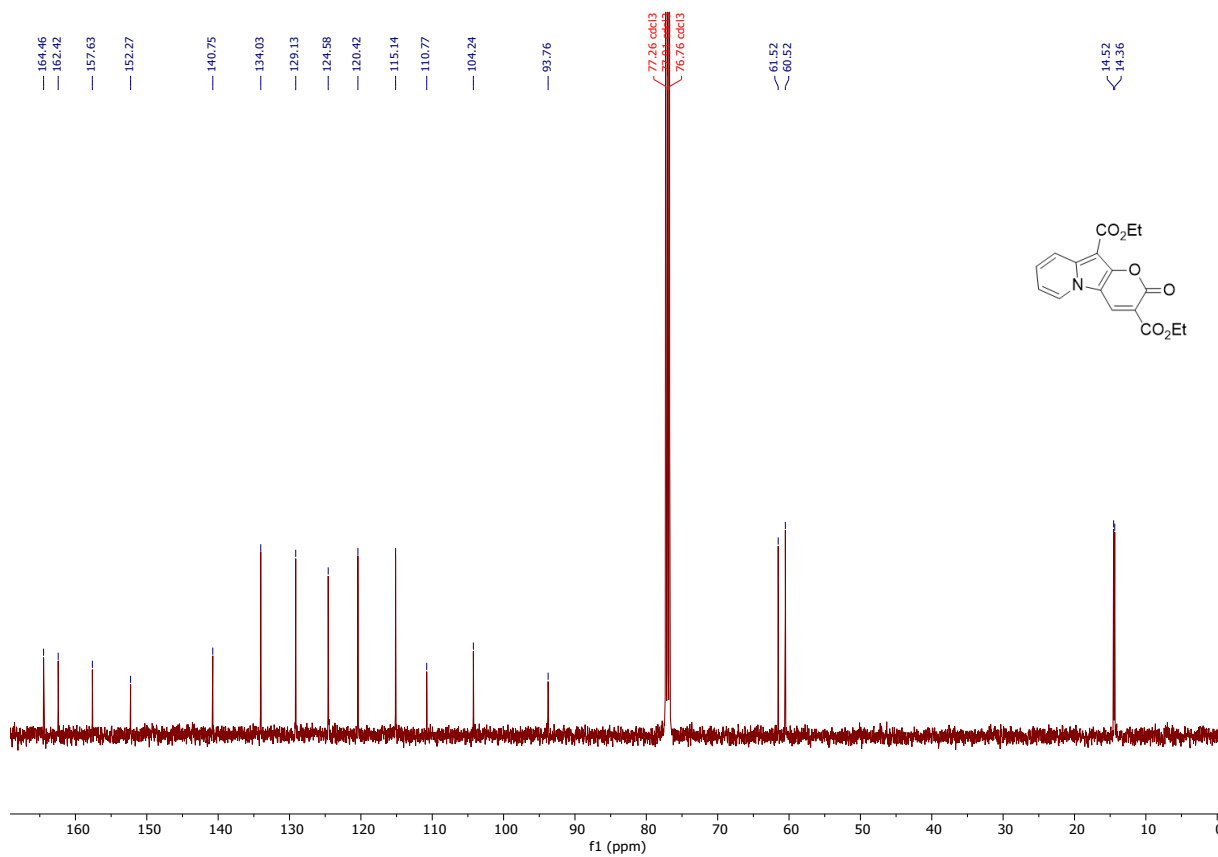
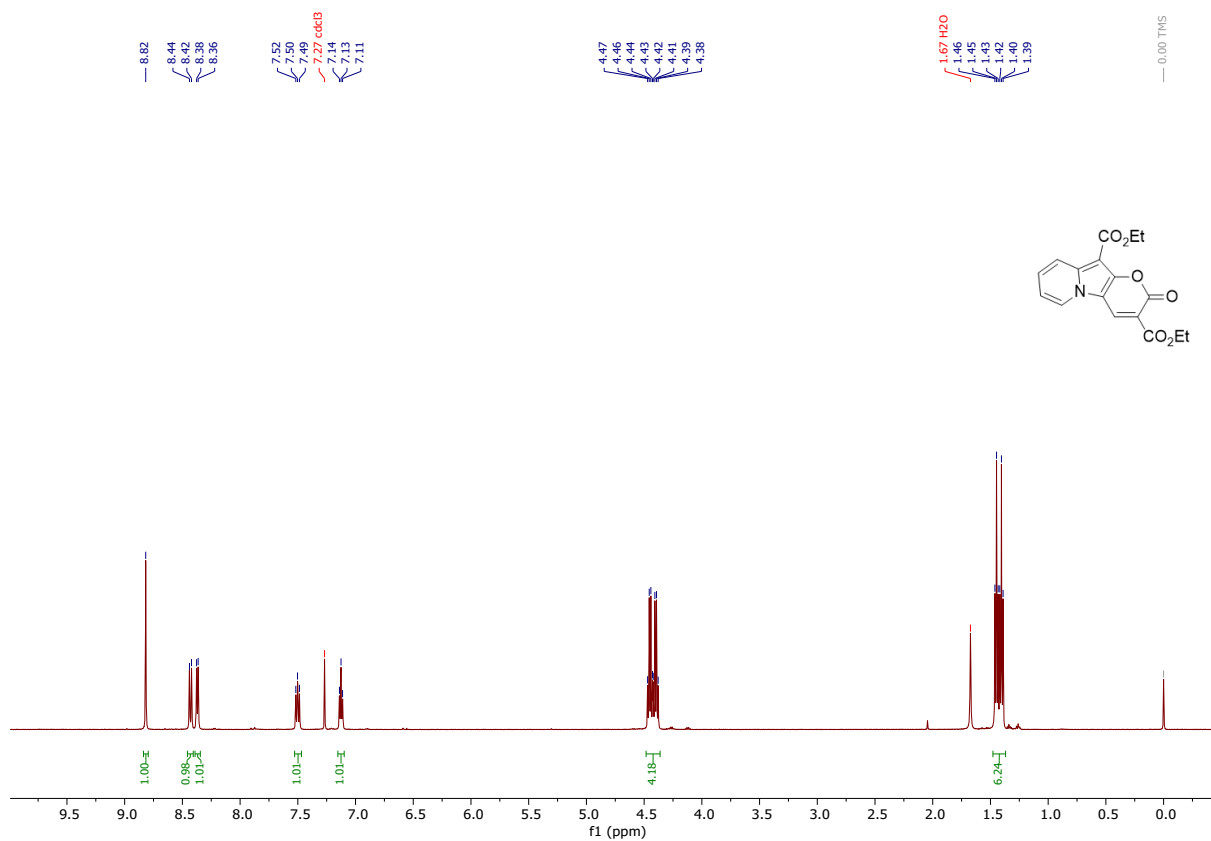
2f



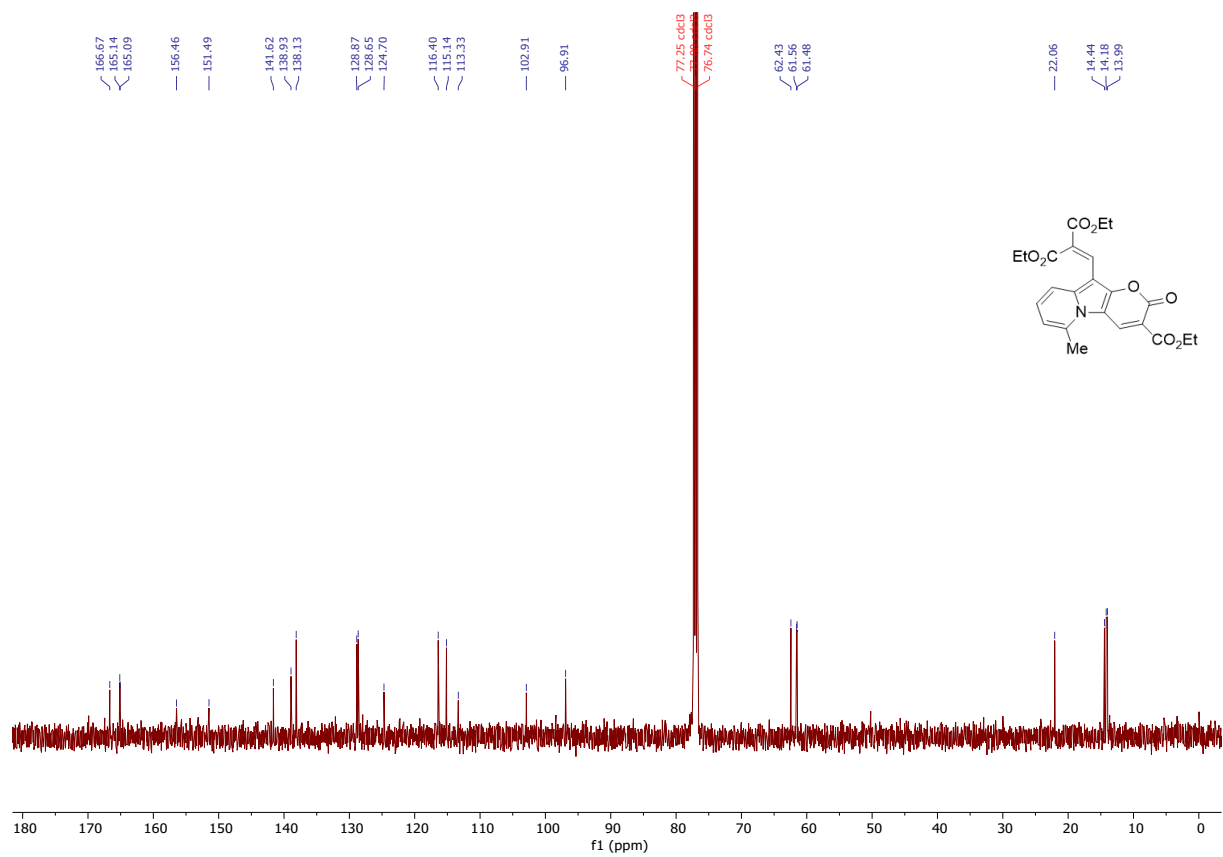
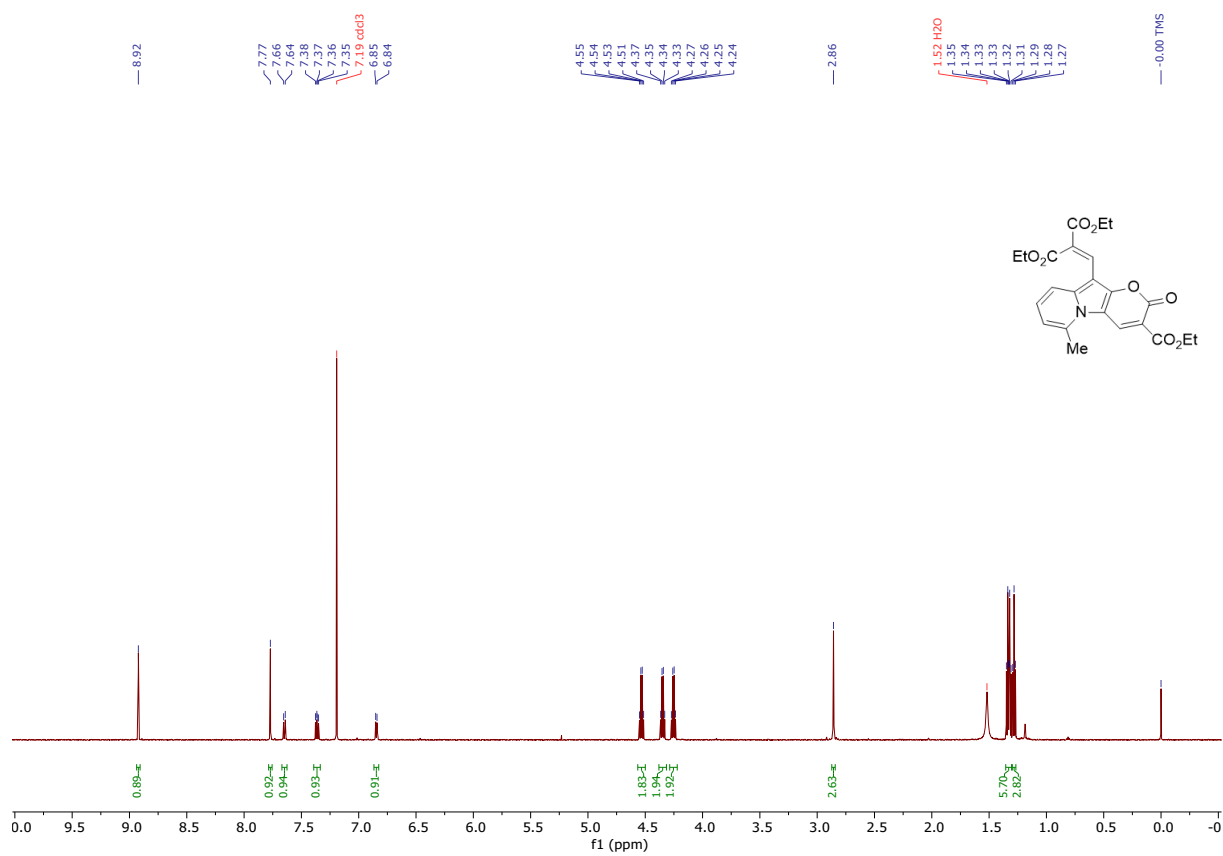
2g



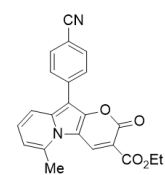
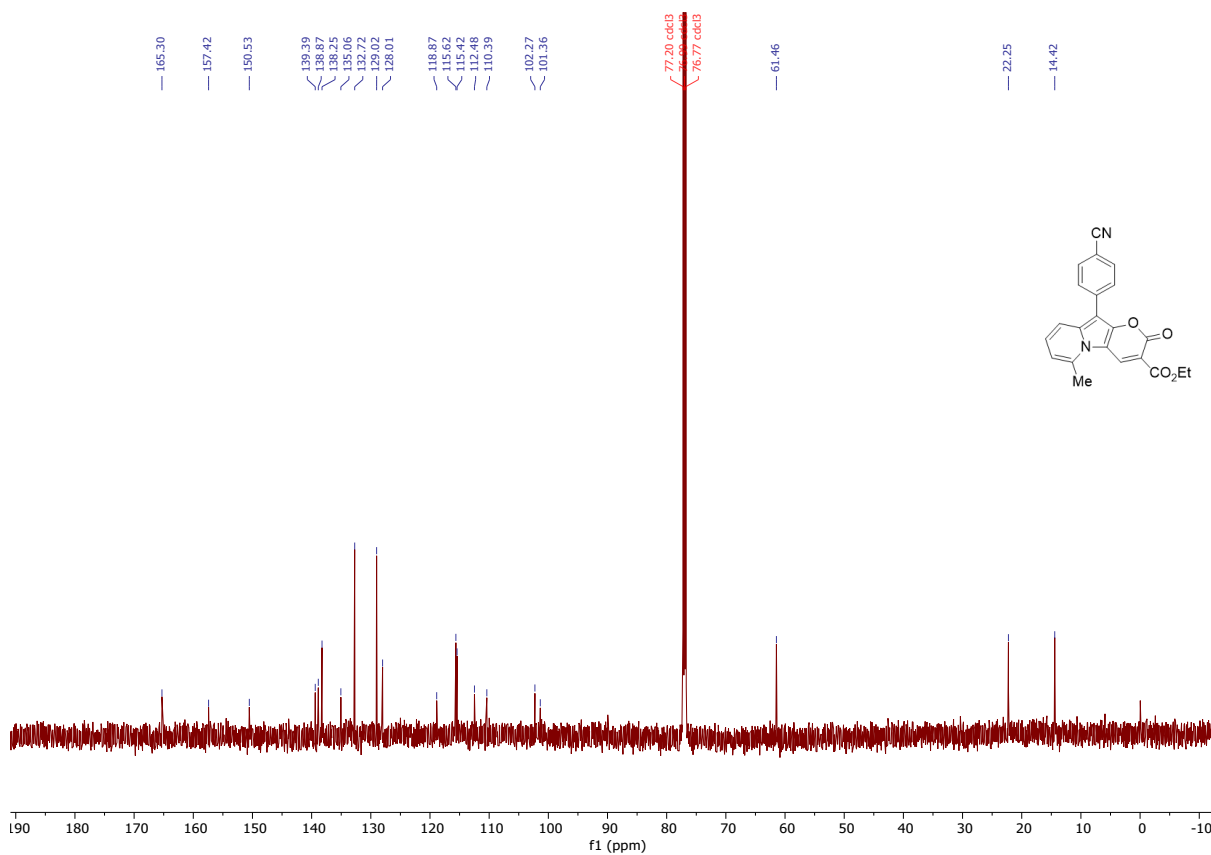
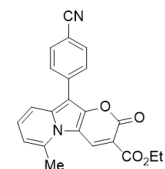
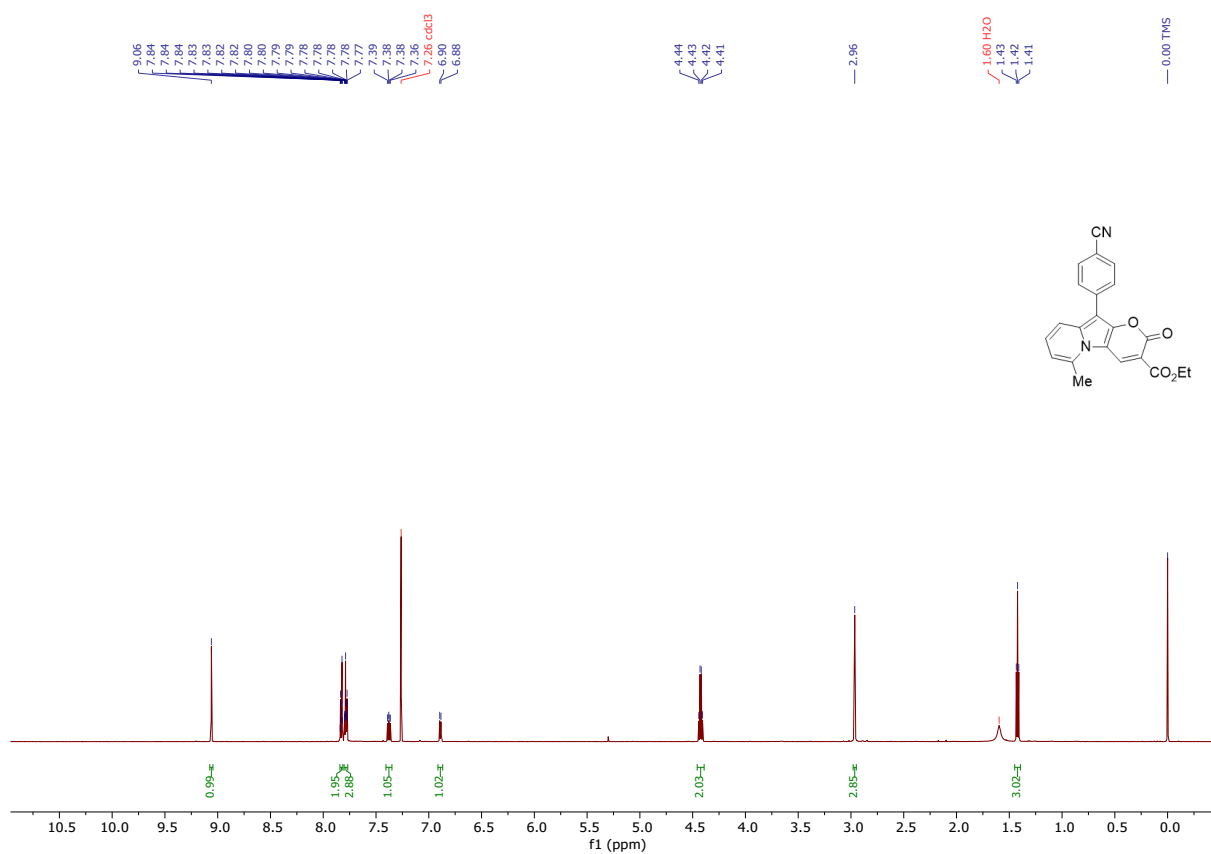
2h



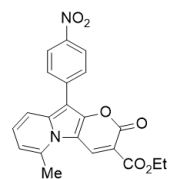
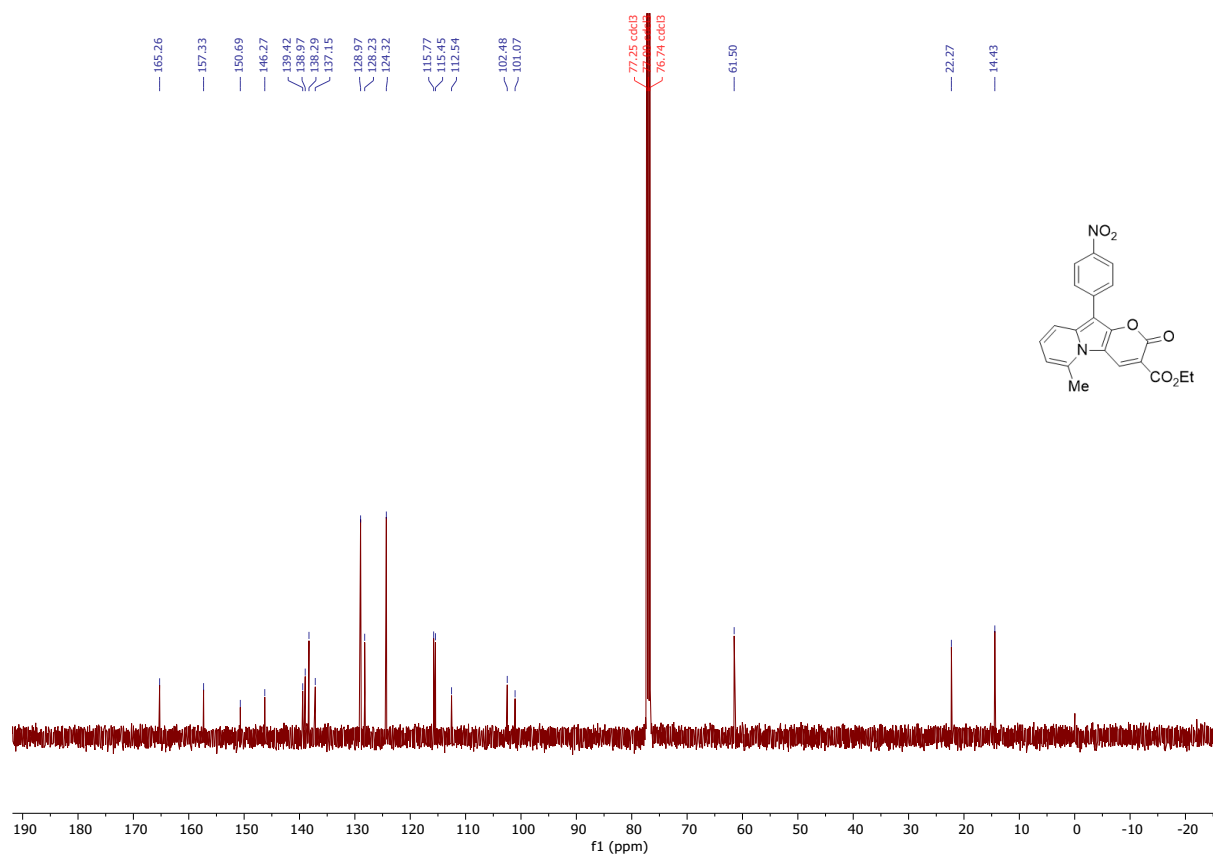
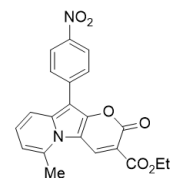
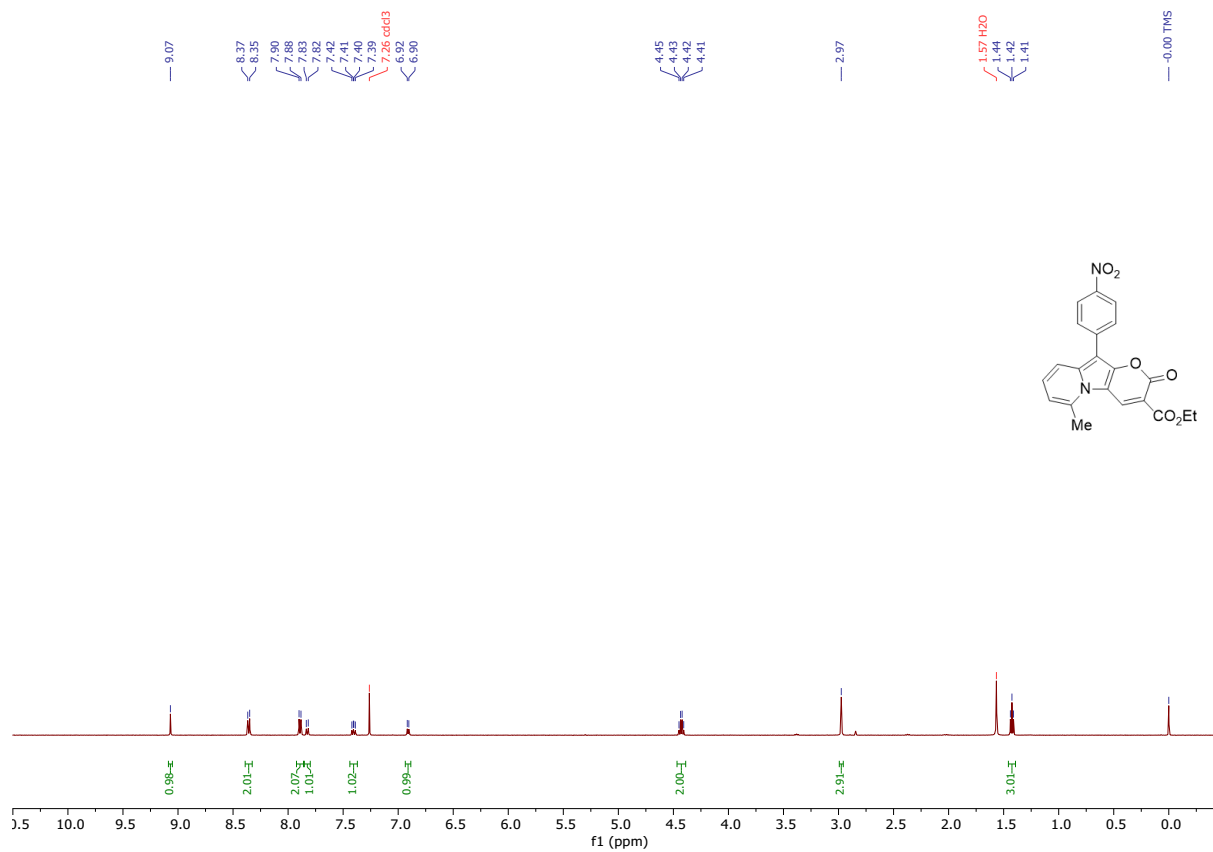
2i



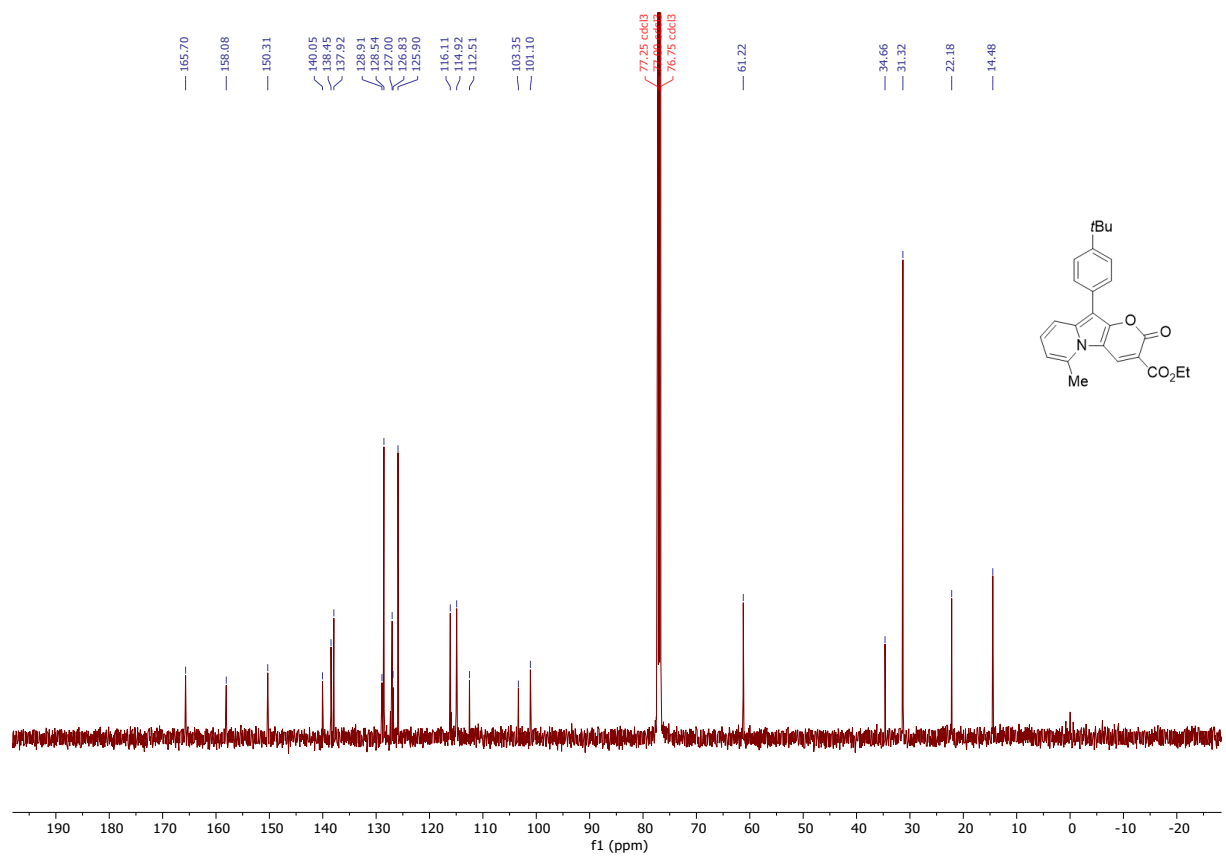
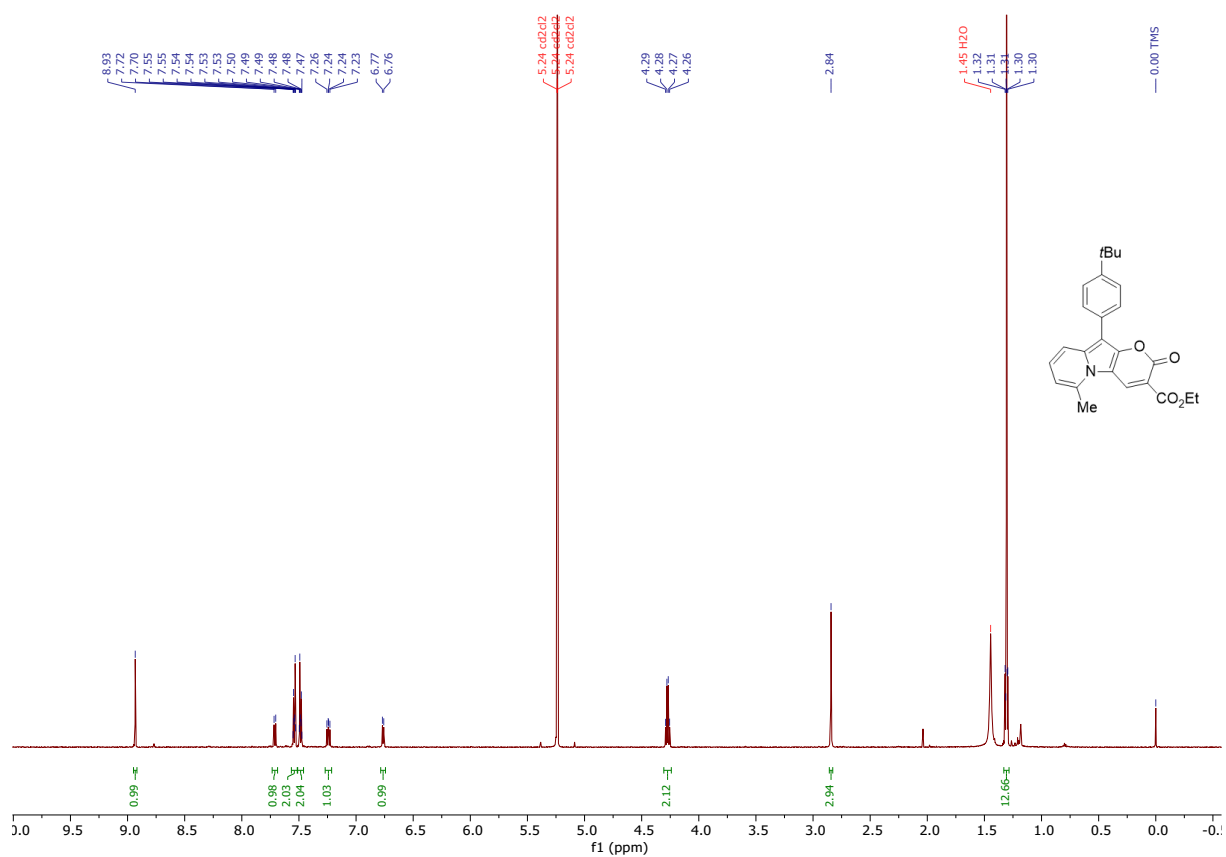
3aa



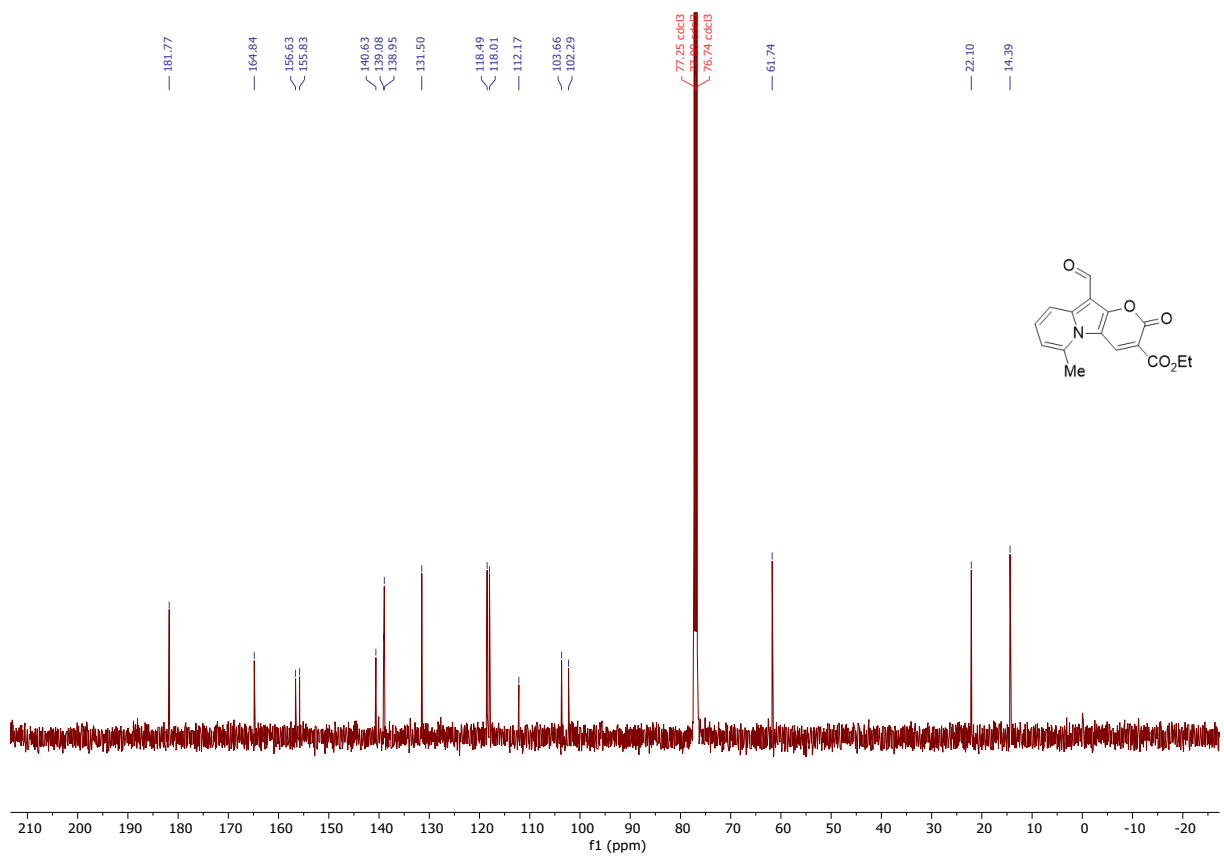
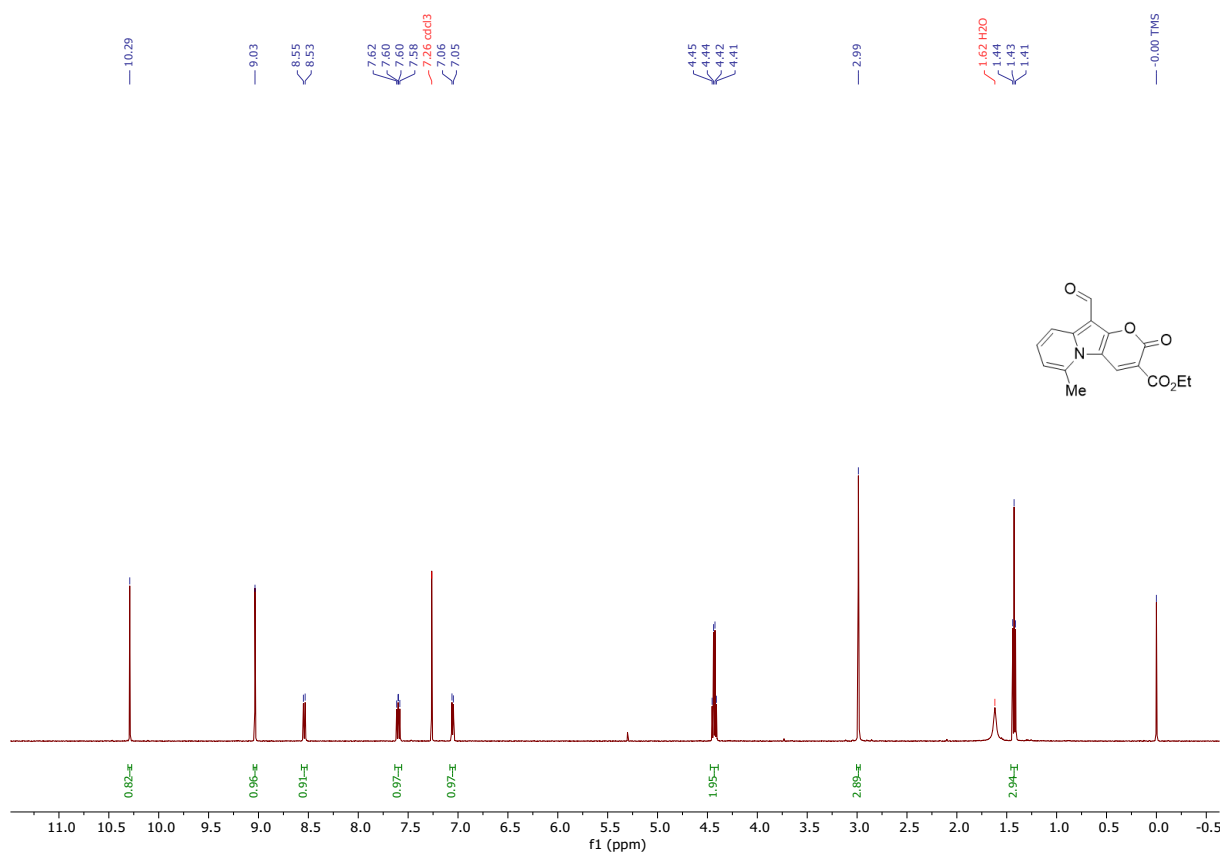
3ab



3ac



4a



6a

